ESR Investigation of Some Free-Radical Adducts

by

Richard Peter Kozloski

Thesis submitted to the Graduate Faculty of the

Virginia Polytechnic Institute and State University

in partial fulfillment of the requirements for the degree of

DOCTOR OF PHILOSOPHY

in

Chemistry

APPROVED:

R E Dessy

Dr. R. E. Dessy, Chairman

Alan F. Clifford

Dr. A. F. Clifford

Paul E. Field

Dr. P. E. Field

G V Gibbs

Dr. G. V. Gibbs

M A Ogliaruso

Dr. M. A. Ogliaruso

January 1977

Blacksburg, Virginia

To My Parents

ACKNOWLEDGEMENTS

I would like to thank Professor Raymond E. Dessy for his aid and financial support, along with my fellow graduate students for their comradery and help. The unselfish aid and encouragement of Dr. Paul J. Krusic was truly in the highest traditions of science.

In particular I would like to thank my parents, without whose aid and encouragement my career would not have been possible.

TABLE OF CONTENTS

LIST OF TABLES

LIST OF FIGURES

INTRODUCTION

Although electron spin resonance spectroscopy was discovered almost thirty years ago, it is only in the last several years that chemists have been able to observe conveniently unstable free radicals in a liquid media. In 1960 Fessenden and Schuler[1] succeeded in observing the esr spectra of some alkyl free radicals by the radiolysis of several alkanes with a 2.8-MeV electron beam. The narrow esr lines that were obtained were a considerable improvement over earlier work done on solid state materials. However, the nonselective bond breakage and hard x-ray scattering intrinsic to the technique prevented its widespread use.

Dixon and Norman published a more practical method in 1963[2]. By combining a flow of dilute hydrogen peroxide with another of a solution of Ti^{3+} in aqueous acid, a source hydroxy free radicals was obtained, which was used to derive a series of free radicals from alcohol substrates by hydrogen atom abstraction. The procedure was further improved by Livingston and Zeldes, who replaced the stream of Ti^{3+} solution with a high intensity ultraviolet lamp to decompose the stream of hydrogen peroxide into hydroxl free redicals.[3] The capability of running in a neutral medium allowed them to resolve the hydroxyl proton hyperfine splittings of the radicals obtained from alcohols by α-hydrogen atom abstraction.

The use of di-t-butyl peroxide instead of hydrogen peroxide by J. Q. Adams[4] opened up the use of free-radical precursors that had

been previously excluded because they were only soluble in nonpolar solvents. The ultraviolet irradiation techique was brought to the present state of the art by Krusic and Kochi, who introduced the use of cyclopropane and ethane as solvents and the use of sealed tubes rather than flow systems.

The studies of various silyl free radicals by Krusic and Kochi[5] suggests to us that this technique could be used to obtain organometallic species of unusual oxidation states. However, our abstraction of hydrogen atoms from such transition element compounds as $HMn(CO)_4$, $[Fe(CO)_3SCH_3]_2$, and $(CH_2{=}CHCH{=}CH_2)Fe(CO)_4$ resulted in the build-up of wide stable singlets which masked any other signals.

Attempts to investigate fluorinated silyl radicals ended with the discovery of work that had been previously done in this area[6], but only after the independent synthesis of the dimethylfluorosilyl radical by hydrogen atom abstraction from dimethylfluorosilane. This experience proved to be of value since it provided us with an interesting species to add across unsaturated olefins.

After learning that free-radical addition to sulfur tetrafluoride invariably leads to a cis product[7], an attempt was made to observe whether the free-radical intermediate was in a cis or a trans configuration, which rearranged on quenching. The product of addition of the t-butoxy free radical to sulfur tetrafluoride dissolved in cyclopropane gave an esr signal, which showed the intermediate to be in the cis configuration. Attempts to add other free-radical species to sulfur tetrafluoride soon ended when we

discovered that Morton and Preston[8] had published such a study a week prior to our initial discovery.

Our redirected efforts into the area of free-radical adducts resulting from the addition of free radicals to unsaturated compounds is the topic of the following thesis. The main purpose of this work was

1. To explore the chemistry of free-radical addition to olefins,
2. To study the hyperfine splitting constants of various free-radical adducts as we systematically changed the free-radical species from which they were generated,
3. To provide experimential details of photoirradiation esr.

PART I

ESR STUDIES OF ADDUCTS FORMED BY THE ATTACK OF SILYL RADICALS ON PERFLUOROALKENES

INTRODUCTION

The advent of techniques for observing the esr spectra of unstable free radicals in liquid media have made the determination of the isotropic splitting constants of these species a much simpler task it had been previously. This technological advance has allowed us to study the hyperfine splitting constants of a number of perfluoro-olefins free-radical adducts.

The successful use of the McConnell equation and its modifications[9] in describing α-proton hyperfine coupling has made it one of the mainstays of esr spectroscopy. The equation has proved very successful in describing the mechanism of spin density transmission to the α-proton via the polarization of the hydrogen s electrons by the p orbital holding the unpaired electron on the carbon atom, where

$$a_H = Q^H_{CH}\,\rho_C$$

a = proton coupling constant

Q = semiempirical constant

ρ = unpaired electron density on carbon

When this type of semiempirical equation is applied to a F^{19} coupling constants, it fails utterly. If we invoke the same mechanism of spin polarization that we used in the α-proton case we get negative spin densities at the fluorine nuclei. However, an early

study of the trifluoromethyl free radical[10] showed that its F^{19} hyperfine splitting constant was positive.

In order to account for this, a number of authors proposed McConnell-type equations, which incorporated additional terms.[11]

Their results can be summarized in the following equation,

$$\alpha(F^{19}) = Q_C^F \rho_C^\pi + Q_{CF}^F \rho_{CF}^\pi + Q_F^F \rho_F^\pi$$

where in addition to the original $Q_C^F \rho_C^\pi$ term (to account for fluorine s electron spin polarization by the carbon pi electron) there are two new terms. The first new term ($Q_{CF}^F \rho_{CF}^\pi$) includes the effects of off-diagonal pi spin density in polarizing the fluorine s electrons; the second new term ($Q_F^F \rho_{CF}^\pi$) takes into account the effect of fluorine pi spin density in polarizing the fluorine s electrons.[11] The proposed values for the Q's used in the above equation vary over an extremely wide range. This is believed to be due in large part to the nearly linear relationship between the pi spin density on the carbon and fluorine atoms found in most of the systems studied thus far.

This present inability to obtain good values for these Q's makes these multiterm equations little better than a one term equation using an effective Q. However, the more sophisticated approaches to the problem of F^{19} hyperfine coupling at least begin to provide us with some insight into the nature of F^{19} hyperfine coupling.

Even though it is hard to define quantitatively a relationship between the spin density on the carbon atom and the fluorine hyperfine coupling constant, there is a simple qualitative relationship

between the degree of nonplanarity of the free radical and the number of α fluorine atoms present.

In their classic studies on the $\cdot CH_nF_{3-n}$ free radical series, Fessenden and Schuler showed that as the number of fluorine atom substituents was increased, the degree of nonplanarity of the fluorinated free radicals increased.[10] Thus, whereas the methyl free radical is planar, the trifluromethyl free radical is only about two degrees from being completely tetrahedral. This is in accord with Pauling's theory that the greater the number of electronegative groups the greater the nonplanarity of the free radical.[12]

Their work also showed that as we go from $\cdot CH_2F$ to $\cdot CF_3$ and as the free radical becomes less planar, the absolute values of the fluorine hyperfine splitting constants increase (64.3 to 142.4 gauss).

It has been suggested that as the free-radical planarity decreases the fluorine hyperfine coupling of any adjacent trifluoromethyl groups should decrease since any β-fluorine interaction arising from hyperconjugation should decrease.[13] In this thesis we explore the effects on the α-fluorine and trifluoromethyl group coupling constants as we change the degree of nonplanarity of some fluorinated free radicals by means of steric effects.

In the past several years extensive research has been carried out in the area of the preferred conformations of free-radical adducts. Interest in this area is particularly strong where intermediate bridged structures have been proposed to account for the stereochemistry of the products.[14,15]

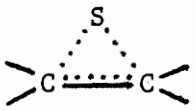

Figure 1. Structure of bridged free-radical intermediate.

In view of this it would be especially interesting to investigate and compare the preferred conformations of fluorinated free radical adducts to that of the hydrocarbon species that have been reported.

EXPERIMENTAL

Sample Preparation

All gasses purchased from commercial sources were degassed by freezing and thawing using liquid nitrogen. This procedure was necessary for efficient bulb-to-bulb transfer of the gas as well as for preliminary removal of contaminating oxygen. From the quantity of gas pumped off on the first freeze-thaw cycle, it would appear that most small gas cylinders are not pumped down before being filled. All other chemicals used in the study were appropriately degassed by freezing and thawing.

The quantities of chemicals to be sealed in a quartz tube for photoirradiation were measured out using a simple Bourdon vacuum gauge graduated in inches of mercury. A vacuum manifold of about 425 ml capacity served as a suitable compliment to the sensitivity of the gauge.

The typical ratio of the reactants used was one volume of di-*t*-butyl peroxide to one volume of the secondary radical source (e.g., Me_3SiH) to one volume of olefin to six volumes of cyclopropane, all measured as gasses.

Each of the components was transferred to a one liter bulb equipped with a cold finger after being measured out. The mixture was then frozen and thawed three times to remove any remaining traces of oxygen. Freezing and thawing in the one liter bulb proved to be far superior to the literature method[16] of freezing and thawing in

the ESR sample tube since the large volume of the bulb allowed most of the sample to vaporize when it was heated in the thaw portion of the cycle. This technique might be more aptly described by the term evaporation-condensation degassing than freeze-thawing. After degassing, the components were distilled bulb-to-bulb into a Suprasil[16] quartz sample tube which was about 20 cm in length. The lower Suprasil portion was joined to the tube with a borosilicate-quartz graded seal and had an I.D. of 3.6 mm and a O.D. of 5.0 mm. Suprasil quartz was selected for the lower portion of the tube since the normal grade of quartz develops a strong esr signal on prolonged exposure to short wave ultraviolet light as well as becoming more opaque to the ultraviolet light.

After being used, each tube was washed out with hydrofluoric acid, rinsed with water and then with reagent grade methanol. The tube was allowed to drain and was then evacuated to remove any deposits or residues from being baked into the glass during annealing after the tube was refitted with a joint to connect it to the vacuum line. After annealing the tube, the aforementioned cleaning procedure was repeated to remove any residues of asbestos paper from the tube.

Before being run, each sample was cooled in a petroleum ether bath to determine the consolution or freezing point of the contents. This was necessary to avoid accidently working in a two phase system.

Chemicals

The di-t-butyl peroxide (Lucidol Div., Pennwalt Corp.) free-radical precursor was purified by passing it through an alumina column and drying it over 3 Å molecular sieves. The cyclopropane (Matheson) diluent, perfluoropropene (Matheson) and perfluoro-2-butene (Columbia, PCR) olefins were degassed before using.

The triethylsilane was purchased from Columbia Organic Chemicals Co. and was used without further purification. The trimethyl-, dimethyl- and methylsilanes were prepared from trimethylchlorosilane (Columbia), dimethyldichlorosilane (Columbia) and methyldichlorosilane (Columbia) by hydrogenation. The synthetic procedure used is typified by the following synthesis of trimethylsilane.

Trimethylsilane was prepared on a vacuum line by vacuum distilling 28.8 grams (0.265 mol) of trimethylchlorosilane onto 5.31 grams (0.140 mol) of lithium tetrahydroaluminate (Alfa) in 60 ml of dried bis(2-methoxyethyl) ether. The product was distilled into a bulb and then redistilled onto 19.3 grams of silica gel (Fisher) leaving most of the less volatile impurities behind. The trimethylsilane was then transferred to a storage vessel. A quantitative transfer was not attempted in order to avoid desorbing the impurities held on the silica gel. The yield based on Me_3SiCl was 16.2 (82%). Product identity and purity were checked by nmr, infrared and mass spectrometry.

The dimethyfluorosilane used was prepared by adding 18.9 g (0.2 mol) of dimethylchlorosilane (Aldrich) over a period of 40 min to 22.8 g (0.4 mol) of powdered ammonium hydrogen fluoride. The mixture

was stirred and cooled for 80 min under a dry ice condenser. The yield was 10.8 g (69%) based on dimethylchlorosilane. The product identity and purity were confirmed by nmr, infrared and mass spectrometry. The infrared spectrum of the compound gave no evidence of hydrogen chloride.

Electron Spin Resonance

A Varian E-12 electron spin resonance spectrometer equipped with an esr cavity that was modified to admit light was used in our studies. A Varian temperature controller and a specially constructed insert Dewar of Suprasil quartz with low dielectric loss was used to regulate the temperature of the samples. The ultraviolet light for the studies was provided by a one kilowatt mercury capillary lamp employing a Suprasil quartz optical system. Details on the use and construction of the equipment and in particular instruction on how to improve the lifetime and stability of the lamp are contained in the appendix.

The thermocouple probe used to measure the temperature of the sample had to be held above the zone of direct photo-irradiation in the esr cavity since light that directly struck the thermocouple produced abnormally high temperature readings which did not reflect the true temperature at the thermocouple. By the use of dummy samples it was estimated that medium strength photo-irradiation raised the temperature of the sample about five degrees and full strength photo-irradiation raised the temperature about ten degrees. In the case of chemical systems where a fairly rapid chain process mechanism occurred during photo-irradiation, the heat liberated by the reaction is

believed to have increased the temperature of the system another five degrees. Because of the uncertainty in estimating the true temperature of the samples in the studies both the corrected and uncorrected temperatures are given in the results.

Electron Spin Resonance Spectra Simulations

The esr computer simulations that were done using a program based on the program SESRS of Stone and Maki.[17] In order to increase the usefulness of the program we modified it so that all the units of measurement were converted to gauss.

A feature listing the positions of all maxima and minima in spectrum was also added to the program. On running some test spectra this feature allowed us to spot some errors in the positions of the peaks. These errors, which were apparently created by difficulties in rounding off, were reduced to negligible proportions by adding the option of increasing the number of increments into which the spectrum was divided when being calculated.

The versatility of the program was further increased by including the capability of adding several esr spectra together, thus allowing us to simulate esr spectra of mixed radical species. Because of difficulties in preparing comparison photographs of the original and simulated esr spectra, the subroutine that generated vertical and horizontal coordinate lines on the computer plot was removed from the plotting subroutine specifications.

Evaluation of Data

The scaling factors needed to obtain absolute values on the 200 and 400 gauss scales of our spectrometer were obtained by using a 1×10^{-3} molar manganese(II) chloride as a standard. The spectrum used to derive the absolute values of the splitting constants of the manganese(II) chloride standard were obtained by courtesy of Dr. Paul J. Krusic (Central Research Dept., E. I. du Pont de Nemours and Company, Wilmington, Delaware), who ran the spectrum on an esr spectrometer that utilized an nmr water marker for calibration. The distances between the points at which the first and fifth peaks and the second and third peaks crossed the baseline were found to be 376.5 and 188.3 gauss, respectively (9.492 GHz).

Comparisons of old and new data showed that the scaling factors for the latter were larger than the older scaling factors. The differences between scaling factors amounted to about a 1% increase per year and were apparently caused by the aging of our instrument's electrical components. Unfortunately the rate of aging was not always uniform as is evidenced by the fact that the scaling factor changed from 1.057 to 1.061 between 1/21/76 and 3/2/76. By comparing older data to new data we were able to construct a correction chart for partly eliminating this error.

The degree of precision in our data was taken to be the average mean error in a given hfs measured at different points in the spectrum. The average mean error of triplet and quartet hyperfine splitting (hfs) was divided by 3 or 2 respectively when the entire

manifold was measured. In such cases the measurements of the inner lines of the manifold were included in the determination of the average mean error.

More sophisticated treatments of the data, such as the determination of the standard error were not used, since the requirement of randomness in the error was questionable in many instances. In particular it was noted that the hfs measured on one side of some sets of spectra were noticeably different in value from those measured on the other side (under the conditions of resolution used this was not thought to be due to second order effects). The causes of nonrandom error, which affected the precision of our data, were the drifting of the microwave frequency, changes in the non-linearity correction factor (see appendix) and the underlying lines of free-radical impurities. These cumulative errors were apparently sufficient to cause a noticeable discrepancy between the central portions of a few of the experimental and computer-simulated spectra when the spectra were carefully inspected. (Note: Errors tended to accumulate in the central region of the spectra.)

RESULTS

The relative ease in obtaining esr spectra of the systems under study is determined by the kinetics of the systems. The qualitative results for each photo-irradiated system are given below along with its implied kinetics. Following this section, the trends observed in the ESR splitting constants will be discussed.

$Et_3Si\cdot$ Adduct of $CF_3CF{=}CFCF_3$:

A strong, well resolved spectrum was obtained even near room temperature by opening the light source shutter till the projected image of the lamp just began to form. Even under these mild irradiation conditions the esr signal intensity decreased considerably as the spectrum was scanned.

These facts can be explained by a chain process mechanism as illustrated in Figure 2, propagation steps 3 and 4 account for the rapid consumption of silane and olefin. The absence of any lines attributable to the $Et_3Si\cdot$ free radical indicated that the rate constant k_3, which is a measure of the ease of attack of the silyl radical on the olefin, was much larger than the rate constant k_4, which is a measure of the ability of the free-radical olefin adduct to abstract a hydrogen atom from the silane.

Considering the ease in abstracting a hydrogen atom from a silane due to the relatively weak Si-H bond, the relatively low value of the rate constant k_4 must be attributed to the steric hindrance of the free-radical site on the olefin adduct. The effectiveness of

this steric hindrance in slowing reaction rates is illustrated by the low rate constant of the free-radical termination step (step 5), which is apparent from the strong signal obtained by even mild photo-irradiation of the sample.

The lines from a second esr species could be seen between the main groups of lines in the esr spectra. The possibility that they arose from C^{13} or Si^{29} hyperfine coupling can be eliminated on three bases. Their intensity is too great. The width of these lines is about twice that of the lines of the main spectrum and their hyperfine splitting constants do not correspond to any hyperfine splitting constants of the main spectrum

Neither do these lines correspond to the spectrum resulting from photo-irradiating a mixture of di-t-butyl peroxide and $CF_3CF=CFCF_3$. The fact that these "impurity" lines are similar but not exactly the same in the spectrum of the $Me_2SiF\cdot$ adduct of $CF_3CF=CFCF_3$ exclude their being due to an allylic species such as $CF_3CF\cdots CF\cdots CF_2$ which could be formed by the abstraction of a terminal F atom by a silyl free radical.

Since the impurity spectrum had a width of well over 130 gauss we can exclude their being silyl-centered free radical, leaving free radicals with a fluorinated carbon free-radical site as the only likely alternative. The most likely species that fits the above facts is the species formed by the further addition of the initial free-radiacl adduct to another perfluoro-2-butene molecule.

Initiation Steps:

Step 1 $$C_4H_9OOC_4H_9 \xrightarrow[U.V.]{k_1} 2C_4H_9O\cdot$$

Step 2 $$R_3SiH + C_4H_9O\cdot \xrightarrow{k_2} C_4H_9OH + R_3SiH\cdot$$

Where R = Et,Me or H

Propagation Steps:

Step 3 $$R_3Si\cdot + CF_3CF{=}CFCF_3 \xrightarrow{k_3} CF_3(R_3Si)CF\dot{C}FCF_3$$
$$\text{I}$$

Step 4 $$I + R_3SiH \xrightarrow{k_4} CF_3(R_3Si)CFCHFCF_3 + R_3Si\cdot$$

Where $k_3 >> k_4$

Termination Steps:

Step 5 $$I + R' \xrightarrow{k_5} CF_3(R_3Si)CFCFR'CF_3$$

Where R' = C_4H_9O , $R_3Si\cdot$, I

Step 6 $$R' + R_3Si\cdot \xrightarrow{k_6} R_3SiR'$$

Figure 2. General reaction pathway for the addition of silyl free radicals to perfluorinated olefins.

$$CF_3\dot{C}RFCFCF_3 + CF_3CF{=}CFCF_3 \longrightarrow \begin{matrix} CF_3CRFCFCF_3 \\ | \\ CF_3C\dot{C}FCF_3 \end{matrix}$$

Figure 3. Addition of a substituted perfluorobutyl radical to perfluoro-2-butene.

The observation that the ratio of the impurity spectrum to the main spectrum decreased as the sample deteriated and the perfluoro-2-butene concentration decreased is consistent with the above hypothesis.

$Me_3Si\cdot$ Adduct of $CF_3CF{=}CFCF_3$:

Good spectra were easily obtained as in the above system, although the signal-to-noise ratio did not appear to be as good. This is readily explained by the lesser efficiency of the steric hindrance in the trimethylsilyl olefin adduct in preventing free-radical recombination steps. Impurity peaks were observed as in the spectrum of the $Et_3Si\cdot$ adduct of $CF_3CF{=}CFCF_3$.

$Me_2SiH\cdot$ Adduct of $CF_3CF{=}CFCF_3$:

Good, well resolved spectra were not obtained. Difficulties such as the overlapping of multiplets, short lifetimes of the free-radical species and the appearance of free-radical adducts which ultimately resulted from the abstraction of the remaining proton of the Me_2SiH- group on termination products made the system difficult to study. The peaks on the ends of the spectrum were observed to be quintets, showing that the proton on the silyl group had approximately the same coupling constant as the fluorine atoms residing an equal number of bonds away from the free-radical center.

$MeSiH_2$· Adduct of $CF_3CF=CFCF_3$:

Usable spectra were obtained, but only at the cost of good resolution. Fortunately the distribution of the lines in the spectra was such that the splitting constants could be obtained in spite of the low resolution. The build-up of other free-radical adducts occurred as in the spectra of the Me_2SiH· adduct of $CF_3CF=CFCF_3$. Under conditions of high resolution the splitting due to the two protons on the silyl substituent was resolvable.

Me_2SiF· Adduct of $CF_3CF=CFCF_3$:

Since the samples did not deteriorate too rapidly on irradiation, good signal-to-noise ratios were obtained by using fairly intense photo-irradiation. The decreased rate of sample deterioration is attributed to the low rate of hydrogen atom abstraction from the Me_2SiHF by the free-radical adduct being observed (step 3, Figure 2). The low rate of hydrogen atom abstraction from the Me_2SiHF was due to the electronegative fluorine atom on the silane. This ability of fluorine to decrease the proton abstraction rates of silanes was probably the cause of our failure to observe the fluorosilyl radical when we had previously photo-irradiated a mixture of H_3SiF and di-t-butyl peroxide dissolved in cyclopropane. The effect was in accord with the general observation that the rate of hydrogen atom abstraction from hydrocarbons by electronegative free radicals is lessened electronegative substituents were placed adjacent to the hydrogen to be abstracted.[15] This effect is accounted for by the

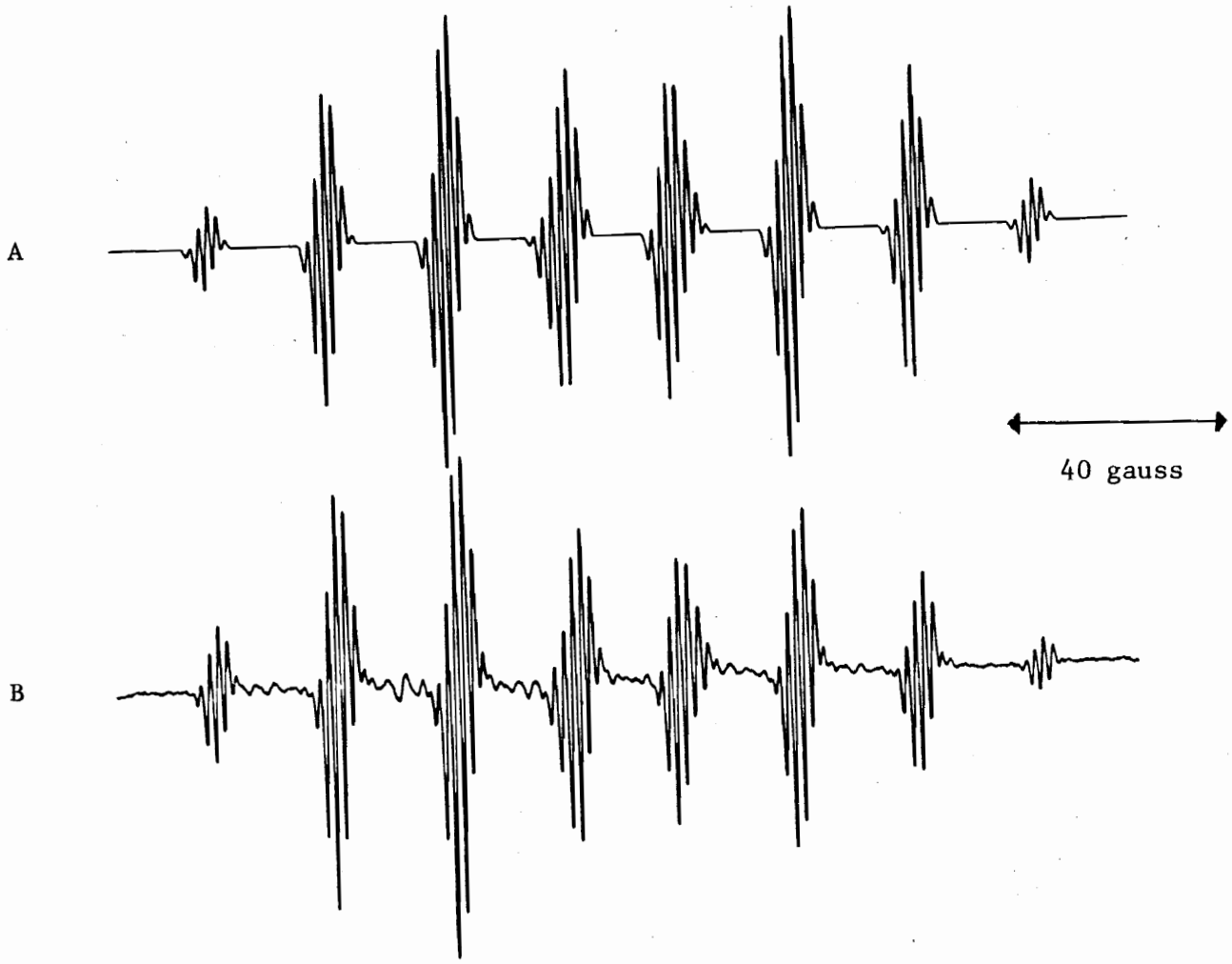

Figure 4. ESR spectra of the dimethylfluorosilyl radical adduct of perfluoro-2-butene. A-experimental spectrum, B-simulated spectrum.

argument that the attacking electronegative species was repulsed by the polarization induced by the electronegative substituent. Impurity peaks were observed as in the other spectra.

$Et_3Si\cdot$ Adduct of $CF_3CF{=}CF_2$:

A good esr signal was obtained, but there was a strong signal due to a second esr species which was also present. The spectrum from this second species was very similar to the esr signal observed on photo-irradiating a mixture of Et_3SiH, $CF_3C{\equiv}CCF_3$ and di-t-butyl peroxide. The resulting $CF_3C(Et_3Si)CF_3$, which was obtained from the photo-irradiation of the above mixture, was fairly stable and gave a strong esr quartet signal with a hyperfine splitting of about 25 gauss.

At ambient temperature, these lines began to show complex asymmetric hyperfine structure. The work of Ingold and co-workers showed, by means of the trimethylsilyl analogue, that the underlying complexity of these lines is due to the existence of two very stable conformers of the free radical.[18]

The resemblance of the above spectra to our "impurity" peaks does not necessarily mean that these peaks were the result of trace amounts of $CF_3C{\equiv}CCF_3$ in the perfluoropropane. Spectra of the above type could have have resulted from some other member of the $CRR'\dot{H}CR''CF_3$ family of free radicals.

$Me_3Si\cdot$ Adduct of $CF_3CF=CF_2$:

A good esr spectrum was obtained, although the same type of impurity as in the spectrum of the $Et_3Si\cdot$ adduct of $CF_3CF=CF_2$ was seen. Spectra virtually free of this impurity were achieved by "burning out" the impurity with ultraviolet irradiation.

$Me_2SiF\cdot$ Adduct of $CF_3CF=CF_2$:

A good spectrum was obtained on photo-irradiation. None of the spectral lines of the impurity that had given us so much trouble in the Me_3SiH and Et_3SiH perfluoropropene systems were apparent in the spectra. However, spectral lines due to the dimethylfluorosilyl radical were present.[6] This clearly shows that the ratio of the rate of attack of the dimethylfluorosilyl radical on the olefin to the rate of attack of the free-radical olefin adduct on the dimethylfluorosilane was less than that of the equivalent rate constant ratios of the other silanes studied. If the conclusion reached in the discussion of the $Me_2SiF\cdot$ adduct of $CF_3CF=CFCF_3$ (page 19), (that the rate of hydrogen atom abstraction from dimethylsilane by the free radical adducts is slow compared to the other silanes studied), is true, it logically follows from the above that the rate of addition of the dimethylfluorosilyl to the perfluoropropene is slower than those rates of the other silyl radicals. This is somewhat surprising since the dimethylfluorosilyl radical is less sterically hindered than the unfluorinated silyl radicals.

Figure 5. ESR spectra of the trimethylsilyl radical adduct of perfluoropropene. A-simulated spectrum, B-experimental spectrum.

The possibility that the trimethyl and triethylsilyl spectra were present in the spectra of their adducts, but buried under the lines of the main spectra was unlikely, since in the case of the spectra of their perfluoro-2-butene adducts they should have been quite visible in the small breaks in the centers of the spectra. Unfortunately the presence of the dimethylfluorosilyl radical could not be confirmed in the spectrum of its perfluoro-2-butene adduct since its spectrum was completely overlapped by the intense sharp lines of the adduct.

$Me_2SiH\cdot$ Adduct of $CF_3CF=CF_2$:

No useful spectra were obtained due to the presence of the forementioned "impurity" spectrum and the rapid consumption of the silane and olefin by a chain process (steps 3 and 4, Figure 2).

$Me_3Si\cdot$ Adduct of $CF_2=CF_2$:

Suitable spectra for study were difficult to obtain due to the narrow temperature range over which spectra could be taken. Above about -100° the sample polymerized to form a cloudy precipitate of polytetrafluoroethylene that produced an interfering esr signal. If the temperature was lowered very much below -100° the attacking silyl radical species did not have enough energy to cross the activation energy barrier and form the free-radical adduct. Thus our studies were limited to about a 20° temperature range.

DISCUSSION

$a^{F\alpha}$ Trends:

The $a^{F\alpha}$ trends observed in the silyl adducts of perfluoropropene and perfluoro-2-butene showed a decrease in the $a^{F\alpha}$ splitting constants as one increased the size of the silyl substituent and forced the radical to become more planar. This is in agreement with the trend recorded for the fluorinated methyl radical series where the $a^{F\alpha}$ splitting constants increased dramatically as the nonplanarity of the radicals increased with further fluorine substitution.[10] This trend has also been noted by other researchers[13], who have changed the degree of planarity of some fluorinated radicals by varying the electronegativity of the groups bonded directly to the free-radical center.

A slight disordering of the $a^{F\alpha}$ trend was seen in the data of the trimethyl and triethyl adducts of perfluoropropene. The precision of the data was insufficent to determine whether the disordering is real.

$a^{F\beta}_{CF_3}$ Trends:

With the exception of the slight disordering of the trimethylsilyl and triethylsilyl adducts of perfluoro-2-butene $a^{F\beta}_{CF_3}$ splitting constants, there was a progressive increase in the $a^{F\beta}_{CF_3}$ splitting

TABLE I

ESR HYPERFINE SPLITTINGS OF THE SILYL ADDUCTS OF PERFLUORO-2-BUTENE[a]

$CF_3\dot{C}FCRFCF_3$	Temperature, °C cor (uncor)	$a^{F\alpha}$	$a^{F\beta}_{CF_3}$	$a^{F\beta}_{CRF}$	$a^{F\gamma}$	$a^{F\alpha}/a^{F}_{CF_3}$
R = $SiEt_3$	+25°(+20°)	63.95 ±0.07[c]	23.80 ±0.05	17.31 ±0.08	1.69 ±.05	2.69
R = $SiMe_3$	- 6°(-13°)	65.83 ±0.07	23.80 ±0.02	18.15 ±0.04	1.48 ±.02	2.77
R = $SiMe_3$	+23°(+16°)	65.78 ±0.19	23.96 ±0.09	18.41 ±0.13	1.61 ±.05	2.75
R = $SiMe_2F$	+31°(+24°)	66.52 ±0.12	22.83 ±0.06	24.73 ±0.20	1.66[b] ±.10	2.91
R = $SiMeH_2$	-30°(-40°)	67.09 ±0.42	22.43 ±0.25	28.32 ±0.27	----	2.99

[a] In Gauss

[b] Hfs of γ-fluorine on the silyl group about the same.

[c] Precision of a given hfs relative to others of the same type in table. Accuracy of hfs is about an additional 1% for α and β fluorine atoms.

TABLE II

ESR HYPERFINE SPLITTINGS OF THE SILYL ADDUCTS OF PERFLUOROPROPENE[a]

CF_3CFCRF_2	Temperature, °C cor (uncor)	a^{F_α}	$a^{F_\beta}_{CF_3}$	$a^{F_\beta}_{CRF}$	$a^{F_\alpha}/a^{F_\beta}_{CF_3}$
R = $SiEt_3$	-50°(-60°)	64.71 ±0.20[b]	23.31 ±0.05	42.29 ±0.20	2.78
R = $SiMe_3$	-64°(-74°)	64.65 ±0.34	23.05 ±0.10	40.66 ±0.14	2.80
R = $SiMe_2F$	-79°(-68°)	65.85 ±0.39	22.22 ±0.16	41.12 ±0.36	2.96

[a] In Gauss

[b] Precision of a given hfs relative to others of the same type in table. Absolute accuracy of hfs is an additional error of 0.3% of the value of the hfs except for the Me_3SiH adduct which has an additional error of 0.5%.

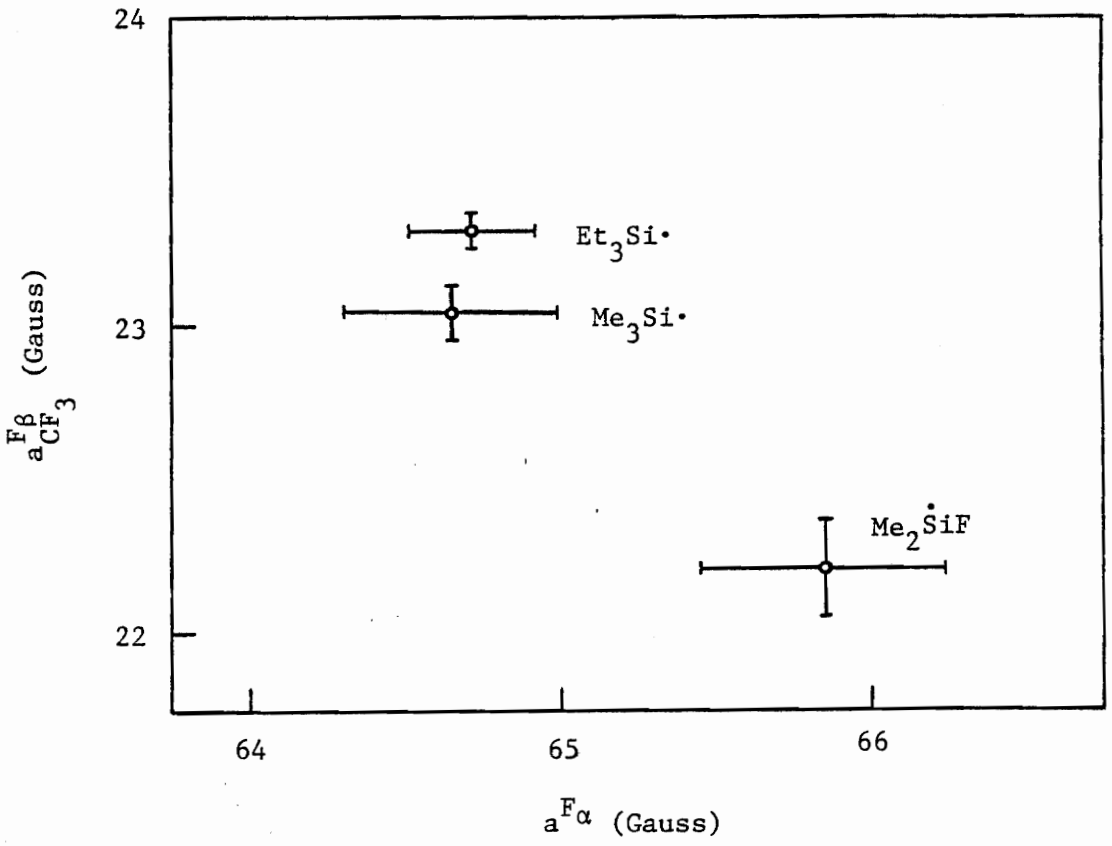

Figure 6. Plot of $a^{F\alpha}$ versus $a^{F\beta}_{CF_3}$ hfs of the silyl adducts of perfluoropropene (labeled with the silyl radicals from which they were derived).

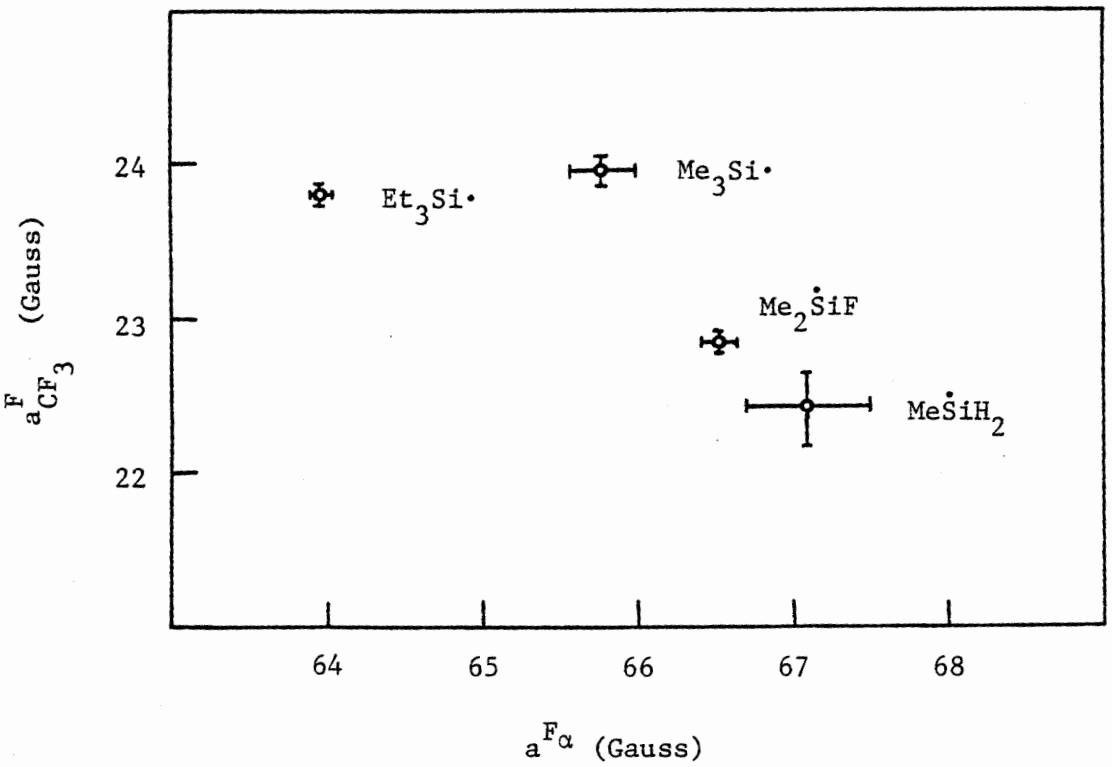

Figure 7. Plot a $a^{F\alpha}$ versus $a^{F\beta}_{CF_3}$ hfs of the silyl adduct of perfluoro-2-butene (labeled with the silyl radicals from which they were derived).

constants as the size of the silyl substituent was increased in both the perfluoropropene and perfluoro-2-butene series. Since spectra were taken on the same day for both the trimethylsilyl and triethylsilyl adducts of perfluoro-2-butene, the degree of precision obtained for the hyperfine couplings was sufficient to determine that this inverse ordering was indeed real.

The observed trend can be explained in terms of molecular orbital theory. By combining the three atomic orbitals of the fluorine atoms of a trifluoromethyl group into a single molecular orbital, we can obtain a pseudo-pi orbital with the same antisymmetric orbital symmetry as a real pi orbital.[19] While admittedly an oversimplification of the β-fluorine spin-coupling process, this model has the virtue of offering us a simple model with reasonably good predictive power.

In the fluorinated systems studied we would expect that as we decrease the degree of steric hindrance provided by the substituent, the free-radical site would more closely approach its natural pyramidal configuration.[10] As the radical assumes a more nonplanar configuration, the overlap of the pi orbital containing the unpaired electron and the pseudo pi orbital of the trifluoromethyl group decreases, resulting in a decrease in the value of the splitting constant associated with the trifluoromethyl group.

The slight disordering of the $a_{CF_3}^{F\beta}$ splitting constants that was observed in the trimethylsilyl and triethylsilyl adducts of perfluoro-2-butene may result from the rotational hindrance of the

trifluoromethyl group by the alkyl groups on the silyl substituent. When the rotation of the trifluoromethyl group becomes hindered, it adopts a preferred conformation, resulting in a change of its hyperfine splitting constant.

These preferred conformations result in a change of the hfs constant because the overlap of the pseudo pi orbital of the trifluoromethyl group and pi orbital containing the unpaired electron is dependent on the dihedral angle between the two orbitals. This relationship between the dihedral angle of the orbitals and the $a^{F\beta}_{CF_3}$ splitting constant has been shown to be $a^{F\beta} = B_o + B_2\rho_\pi\cos^2\theta$,[13] where B_o and B_2 are constants, ρ_π is the unpaired spin density in the pi orbital containing the unpaired electron, and θ is the dihedral angle.

a^{F}_{CRF} Trends:

In the study of hydrocarbon olefin free-radical adducts, equations of the following type have been used to determine the preferred conformation of the substituent relative to the pi orbital containing the unpaired electron.

$a^{H\beta} = A + B\cos^2\theta$

A = 0 to 5 gauss

B = ∿40 to 50 gauss

θ = the dihedral angle between the β-H and the pi orbital containing the unpaired electron

If the group containing the substituent were freely rotating, one would take the weighted average of $a^{H\beta}$ to be about 22 gauss. Therefore, if the $a^{H\beta}$ hfs constant was between 15 and 18 gauss the substituent was considered to be in a preferred conformation parallel to the pi orbital containing the unpaired electron. However, if the value of the $a^{H\beta}$ was between 25 and 30 gauss, the preferred conformation of the substituent was considered to be at 90^{o} to the pi orbital.[16]

An additional test of the conformation would be to study the temperature dependence of the $a^{H\beta}$ splitting constant. As the temperature increases the value of the $a^{H\beta}$ splitting constant approaches the value of the freely rotating group ($\sim$22 gauss). In other words, large values of $a^{H\beta}$ decrease and small $a^{H\beta}$ hfs increase as they approach the free spin value. If a sufficiently large temperature range could be studied the limiting value of $a^{H\beta}$ could be obtained and the value of B in the preceding equation calculated by taking the second term of the equation to be B/2 and A to be zero.[16] Such a procedure would confirm that the value of $a^{H\beta}$ was not due to an abnormally high or low value of B in the equation.

The simple analogous use of such an equation with perfluorocarbons is precluded by the nonplanar nature of fluorine containing free-radical sites. The $a^{H\beta}$ hfs values for a hydrocarbon olefin adduct with a preferred conformation at either 0^{o} or 180^{o} would be expected to be equal, since the conformations are symmetrically equivalent. However, in the perfluorocarbon case the respective

conformations would be expected to have different $a^{F\beta}$ values, due to the large differences in orbital overlap between the two conformations. The value of $a^{H\beta}$ and hence that of B as been shown to vary widely as the degree of nonplanarity at the free-radical site was changed.[20] The replacement of one of the fluorine atoms adjacent to the substituent with a CF_3 group in going from the perfluoropropene series to the perfluoro-2-butene series adds another major perturbation to be accounted for in any conformational analysis of the series.

Even if the above difficulties did not exist, the low degree of symmetry of the free radicals, which includes even the presence of interconvertible erythro and threo isomeric forms for the adducts of perfluoro-2-butene, produces a large number of possible conformers from which to choose. The lack of information on the degree of nonplanarity of the free radicals makes it difficult even to determine the exact nature of the conformers. However, the possibility exists that for a given series of substituents on a given perfluoro-olefin, orderly changes in the $a^{F\beta}_{CRF}$ values may be seen as the size of the substituents is decreased, and conformations that were demanded by the steric hindrance of the larger substituents are replaced by free rotation or conformations based on incipient bonding between the substituent and the unpaired electron.

Upon examination of Table I, we can readily see that as we decrease the degree of steric hindrance (Et_3SiH, Me_3SiH, Me_2SiHF, $MeSiH_3$) in the perfluoro-2-butene series, the $a^{F\beta}_{CRF}$ of the fluorine

atom adjacent to the substituent increases (17.31, 18.41, 24.51, 28.32 gauss). The positive temperature coefficient of 0.01 gauss/degree (-6°C to +23°C) that was obtained for the $a_{CRF}^{F\beta}$ of the trimethylsilyl adduct of perfluoro-2-butene is in agreement with the above finding; that is, as the $C(CF_3)RF$ group is made freer to rotate, the $a_{CRF}^{F\beta}$ hfs increases.

However, on decreasing the degree of steric hindrance (Et_3,SiH, Me_3SiH, Me_2SiHF) in the perfluoropropene series the $a_{CRF}^{F\beta}$ values which resulted (42.29, 40.66, 41.12 gauss), tended to show if anything a slight decrease. (Note: the $a_{CRF}^{F\beta}$ values of the trimethylsilyl and dimethylfluorosilyl adducts of perfluoro-propene are not known with sufficent accuracy to be completely certain of their relative ordering. The narrow spread of $a_{CRF}^{F\beta}$ values, which were observed for the silyl adducts of perfluoropropene, greatly limited the significance of any trend, which could be observed, since other secondary parameters such as changes in the bond distances and angles near the site of the substituent also affected the hyperfine splitting values as well as the changes in the conformation. About 42 gauss may well be an upper limit for this class of adducts.

A subtle alternative to our interpretation of the perfluoropropene results would be that the initial free-radical adduct goes on to attack another olefine molecule. Although this would explain the small range of $a_{CRF}^{F\beta}$ values; it fails to explain the normal range of hfs values observed in the other fluorine couplings.

$a_{CF_3}^{F\gamma}$ Trends:

The generally accepted mechanism of long range spin coupling is the polarization of the spins of the electrons which form the bonds between the two magnetic dipoles of interest.[21] The small range of hfs values that is observed for the γ-fluorines on the trifluoromethyl group farthest from the free-radical site suggests that the transmission of spin density along the carbon backbone of the adduct is essentially unaffected by any change in conformation induced by changing the size of the silyl substituent. However, this should not be taken to mean that a complete change in the class of substituent, such as going to a carbon or a sulfur centered substituent, would not result in a significant change in the $a^{F\gamma}$ values.

$a^{F\alpha}/a^{F\beta}_{CF_3}$ Trends:

By taking the ratios of $a^{F\alpha}$ to $a^{F\beta}_{CF_3}$ we obtained a factor that is independent of the calibration of our instrument. This factor is a good measurement of the degree of steric hindrance in our adducts since the family of lines, which correspond to these ratios on a $a^{F\alpha}$ versus $a^{F\beta}_{CF_3}$ plot, is almost perpendicular to the direction of the trends of the $a^{F\alpha}$ and $a^{F\beta}_{CF_3}$ hfs, which we have observed. The plotting of these ratios (Figure 8) not only gives a good ordering of the degree of steric hindrance in the perfluoro-olefin series, but also shows the lesser degree of steric strain in the perfluoropropene series as compared to the perfluoro-2-butene series.

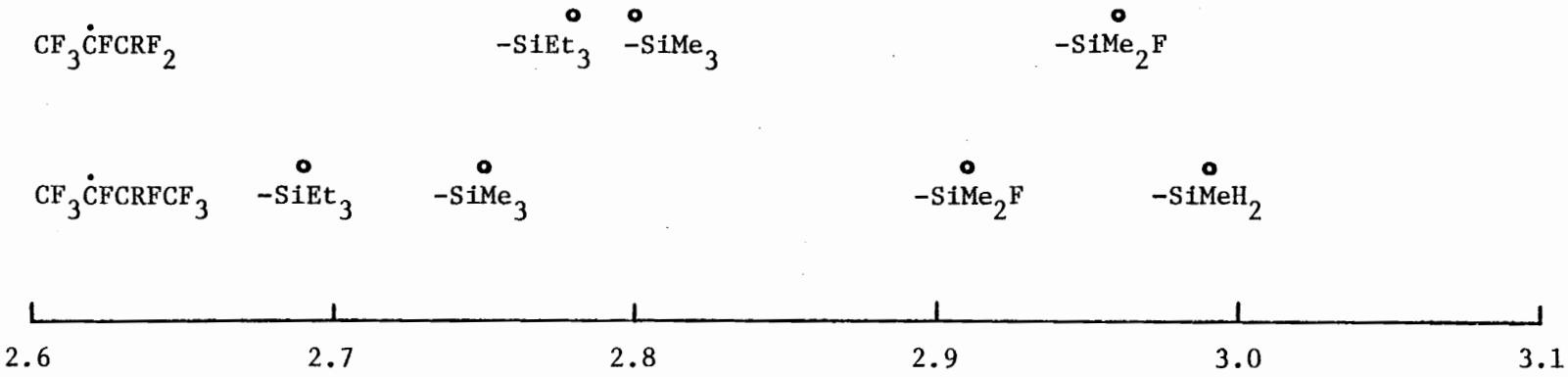

Figure 8. Plot of $a^{F_\alpha}/a^{F_\beta}_{CF_3}$ ratios for the silyl perfluoro-olefin adducts.

CONCLUSIONS

Our study of the silyl free-radical adducts of perfluoro-2-butene and perfluoropropene have shown that as one varies the size of a given class of substituents on the perflorinated free-radical adducts, the major hyperfine splittings tend to change in a regular manner.

The a^{F_α} hyperfine splittings tended to decrease as the planarity of the free radicals was increased by the steric strain induced by the silyl substituents. This result is in accord with the work of Lloyd and Rogers[13], who had varied the degree of planarity of some fluorinated radicals by changing the electronegativity of the substituents at the free-radical center.

The a^{F_β} hyperfine splittings, we observed, tended to increase as the size of the silyl substituents was increased. This in agreement with the expected increase in the degree of overlap between the pseudo pi orbital of the CF_3 group and the pi orbital containing the unpaired electron, as the radical is made more planar.[19] This result is also in agreement with the above mention work of Lloyd and Rogers. Our results establish, however, that the results observed by these other workers, were indeed the result of changes in free-radical planarity and not the result of a redistribution of spin density by the electronegativity of the substituents per se.

Even though no simple interpretation of the $a^{F_\beta}_{CRF}$ hfs constants was attempted, a distinct trend toward lower $a^{F_\beta}_{CRF}$ hfs was observed

when the size of the silyl substitents was increased in the perfluoro-2-butene series. The relative small range in the $a^{F_\beta}_{CRF}$ hfs constants observed in the silyl adducts of perfluoropropene made it difficult to come to any conclusion regarding a trend.

The remote γ-fluorine hfs constants of the perfluoro-2-butene series remained relatively constant for the entire range of silyl substituents.

PART II

ESR STUDIES OF ADDUCTS FORMED BY THE ATTACK OF CR_2OH RADICALS ON PERFLUOROALKENES

INTRODUCTION

The successful experiments with the silyl adducts of perfluoro-olefins prompted us to find other classes of radicals which might add to perfluoro-olefins. The extensive amount of esr research that had been done on free radicals derived from alcohols by hydrogen atom abstraction[22-24], drew our attention to them as a possible class of substituents for our studies. When a primary or secondary alcohol is attacked by a hydroxy or t-butoxy free radical, one of the protons on the same carbon as the hydroxyl group is abstracted. The CR_2OH radicals formed by the hydrogen atom abstraction were found to readily add to the perfluoro-olefins.

Although the addition of alcohol derived free radicals to olefins does not seem to have been studied by esr, we found that an extensive literature had developed concerning its use as a synthetic method. Alcohols were found to have been added to both hydrocarbon and perfluoro based olefins by such diverse means as ultraviolet light, gamma irradiation and organic peroxides.[25-28] The hydroxyalkyl group, which was added, provides a convenient route to the manufacture of alkenes, haloalkanes, esters, etc.

EXPERIMENTAL

Sample Preparation

The same procedures as in Part I were used.

Chemicals

The methanol, ethanol and isopropanol, which were used, were either reagent or spectrograde in quality. All the alcohols were dried over 3 Å molecular sieves prior to use. The di-t-butyl peroxide, cyclopropane and perfluoro-olefins were treated as described in Part I.

Electron Spin Resonance

The same procedures as in Part I were used.

Electron Spin Resonance Spectra Simulations

The same program as in Part I was used. The reduction in the intensity of the "central line" of the "triplet" splitting, in the simulation of the spectra of the perfluoropropene adducts of the hydroxyalkyl radicals was achieved by adding a subspectrun of opposite phase to the main spectum.

Evaluation of Data

The same procedures as in Part I were used.

RESULTS

The qualitative results and implied kinetics for each system is given below, followed by a discussion of the observed hyperfine splitting constants.

$HO\dot{C}H_2$ and $CH_3\dot{C}HOH$ Adducts of $CF_3CF=CFCF_3$:

Good quality spectra were obtained for all the hydroxyalkyl free-radical adducts of perfluoro-2-butene, with little sign of other radicals being present. All the spectra, which were run at ambient temperatures, showed a decay in signal strength as the spectra were being recorded. This is indicative of an efficient chain mechanism, in which the alcohol and olefin are rapidly consumed. Workers who have studied the free-radical addition of alcohols to acyclic perfluoro-olefins as a synthetic method have found no evidence of telomerization (except for $CF_2=CF_2$) and have reported good yields of the alcohol-perfluoro-olefin addition product for the methanol and ethanol adducts.[26]

$HO\dot{C}H_2$ and $CH_3\dot{C}HOH$ Adducts of $CF_3CF=CF_2$:

Spectra were obtained for each of these systems, but the presence of the t-butoxy-perfluoropropane free-radical adduct in the spectra caused considerable difficulty in extracting data from them. As a photo-irradiation progressed the spectral lines of the t-butoxy adduct became more prominent in the spectra. The presence of additional free-radical "impurities" was noted in the spectra of the methanol and ethanol adducts as their photo-irradiation was continued. These

impurities were presumably generated by the further abstraction of protons from the substituents on the adducts.

In our attempt to analyze these spectra, it was noticed that the central lines (M_I=0, two fluorine nuclei of opposite spin) of the β-fluorine triplet were either weak or were virtually missing. This lead us to the wrong assumption that we were dealing with a selective line widening effect or an abnormally wide doublet. Both of these possibilities were worrisome since the first one implied that the free-radical site was planar and other implied extremely strong hindrance to the free rotation of the CRF_2 group. Computer simulations based on the reduction of the intensities of the M_I=0 lines of the β-fluorine triplet gave reasonably good simulations of the spectra (see Figure 9).

However, we later realized that the spectral lines of the t-butoxy adduct, which appeared close to the central lines of the β-fluorine triplet, could be cancelling a good portion of their intensity. The practice we had developed of photo-irradiating a while before attempting a scan, in order to avoid frequency drift as the sample warmed, may have contributed toward our incorrect assumption by allowing the t-butoxy adduct to become an appreciable part of the spectrum as the alcohol in the sample was consumed.

Figure 9. ESR spectra of the $CH_3\dot{C}HOH$ adduct of perfluoropropene. A-simulated spectrum, B-experimental spectrum.

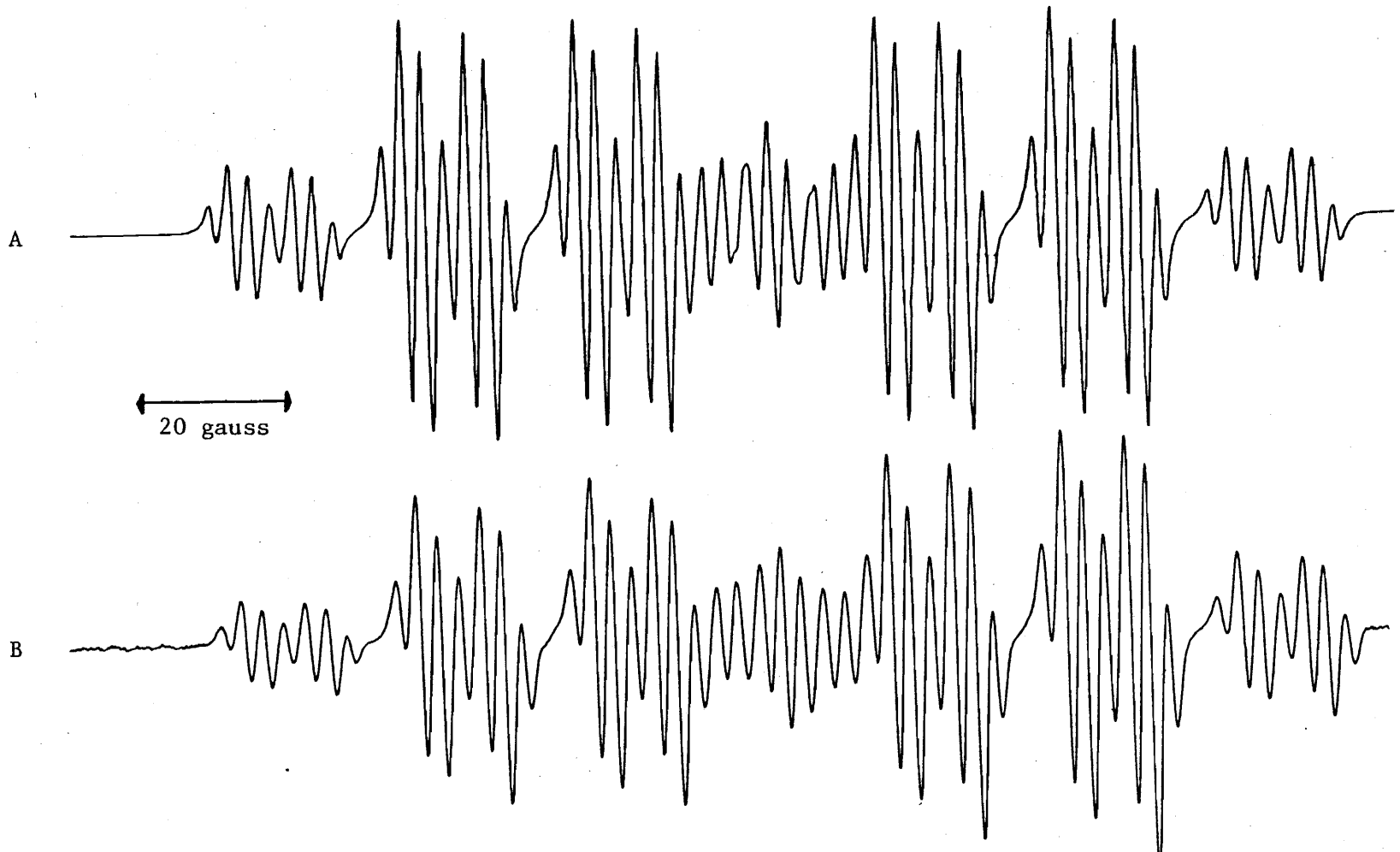

Figure 10. ESR spectra of the $\cdot CMe_2OH$ adduct of perfluoro-2-butene. A-simulated spectrum, B-experimental spectrum.

DISCUSSION

$a^{F\alpha}$ Trends:

The trend toward lower $a^{F\alpha}$ values as the degree of steric strain in the molecule is increased is confirmed by the studies of the perfluoro-olefin adducts of the hydoxyalkyl free-radicals. The degree of error in the data of the perfluoropropene adducts limits their value in making this point.

$a^{F\beta}_{CF_3}$ Trends:

The trend toward higher $a^{F\beta}_{CF_3}$ values as the adduct becomes more planar with increasing substituent size is apparent; however as in the $a^{F\alpha}$ trends the degree of error in the perfluoropropene data makes the trend observed for that series marginal.

$a^{F\beta}_{CRF}$ Trends:

Both the hydroxyalkyl perfluoro-2-butene and perfluoropropane free-radical adducts showed regular monotonic increases in their $a^{F\beta}_{CRF}$ hfs as the size of their substituents was decreased. The perfluoro-2-butene adduct of $CH_3\dot{C}(OH)CH_3$ free-radical showed a temperature coefficient of approximately 0.01 G/°C (between -4 and +26°C) for its $a^{F\beta}_{CRF}$ hfs. This confirms our finding, that the $a^{F\beta}_{CRF}$ hfs increases as the group containing the substituent approaches its free rotation limit.

$a^{F}\gamma$ Trends:

The γ-fluorine hfs were only mildly affected by the variation in the size of the substituents and showed no discernible trends as the degree of steric strain was varied. The γ-fluorine hfs did appear to be effected by the functional class of the substituent that was added however. In the silyl free-radical adducts the range of γ-fluorine hfs varied from 1.52 to 1.69 gauss, but in the hydroxyalkyl free-radical adducts the range was from between 2.44 to 2.74 gauss. Major differences in the electronegativity of substituents apparently causes a change in the spin density transmission on the carbon backbone.

$a^{F\alpha}/a^{F\beta}_{CF_3}$ Trends:

The ratio of the α and β-fluorine hfs gave a good indication of the amount of strain introduced into the radical by the substituent. Using this parameter there were not the irregularities in the ordering of the sizes of the substituents that were reported in Part I, when $a^{F\alpha}$ and $a^{F\beta}_{CF_3}$ were used as independent indicators of the degree of steric strain introduced into the free radical by the substituents.

TABLE III

ESR HYPERFINE SPLITTING OF THE HYDROXYALKYL ADDUCTS OF PERFLUORO-2-BUTENE[a]

$CF_3\dot{C}FCRFCF_3$	Temperature, °C cor (uncor)	a^{F}_{α}	$a^{F}_{\beta}{}_{CF_3}$	$a^{F}_{\beta}{}_{CRF}$	a^{F}_{γ}	$a^{F}_{\alpha}/a^{F}_{\beta}{}_{CF_3}$
R = Me-C(Me)-OH	+32°(+25°)	64.63 ±0.07	23.72 ±0.06	8.61 ±.05	2.74 ±.05	2.72
R = Me-C(H)-OH	+31°(+24°)	65.48 ±0.12	23.55 ±0.06	13.52 ±0.08	2.81 ±.04	2.78
R = H-C(H)-OH	+36°(+24°)	66.21 ±0.36	22.92 ±0.22	21.63 ±0.17	2.44 ±.05	2.89

[a] In Gauss

[b] Precision of a given hfs relative to others of the same type in table. Absolute accuracy is about 1%.

TABLE IV

ESR HYPERFINE SPLITTING OF THE HYDROXYALKYL ADDUCTS OF PERFLUOROPROPENE[a]

$CF_3\dot{C}FCRF_2$	Temperature, °C cor (uncor)	a^{F_α}	$a^{F_\beta}_{CF_3}$	$a^{F_\beta}_{CRF}$	$a^{F_\alpha}/aCF_3^{F_\beta}$
R = Me-$\dot{C}$(Me)-OH	-20(-31)	65.46 ±0.5	22.62 ±0.11	25.74 ±0.26	2.89
R = Me-$\dot{C}$(H)-OH	-20(-32)	65.77 ±0.5	22.60 ±0.06	28.62 ±0.21	2.91
R = H-$\dot{C}$(H)-OH	-73(-86)	66.69 ±0.2	22.30 ±0.11	30.77 ±0.22	2.99

[a] In Gauss

[b] Precision of a given hfs relative to others of the same type in table. Absolute accuracy is an additional 0.3% except for the methanol adduct where the additional error is 0.1%.

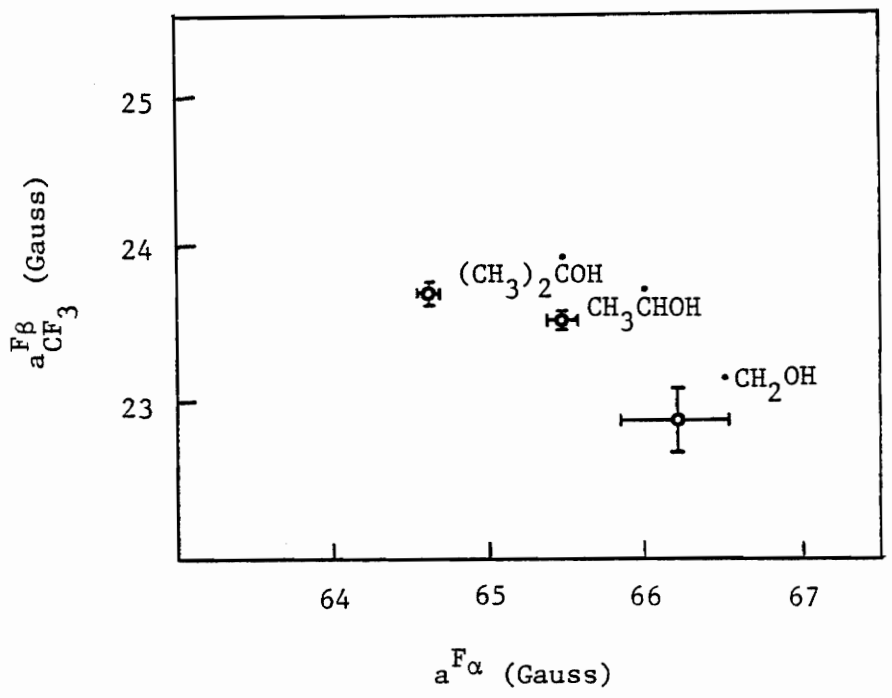

Figure 11. Plot of the $a^{F\alpha}$ versus $a^{F\beta}_{CF_3}$ hfs of the hydroxyalkyl radical adducts of perfluoro-2-butene (labeled with the hydroxyalkyl radicals from which they were derived).

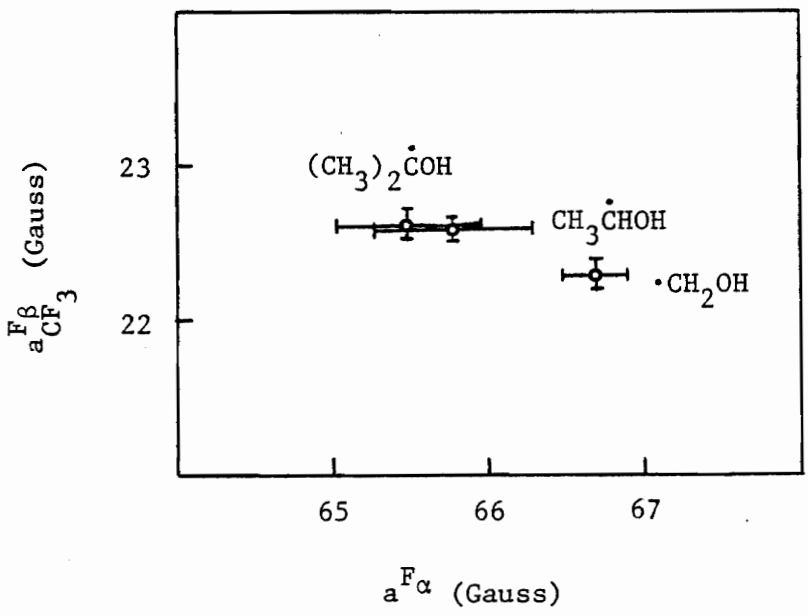

Figure 12. Plot of the a^F versus $a^F_{CF_3}$ hfs of the hydroxyalkyl radical adducts of perfluoropropene (labeled with the hydroxyalkyl radicals from which they were derived).

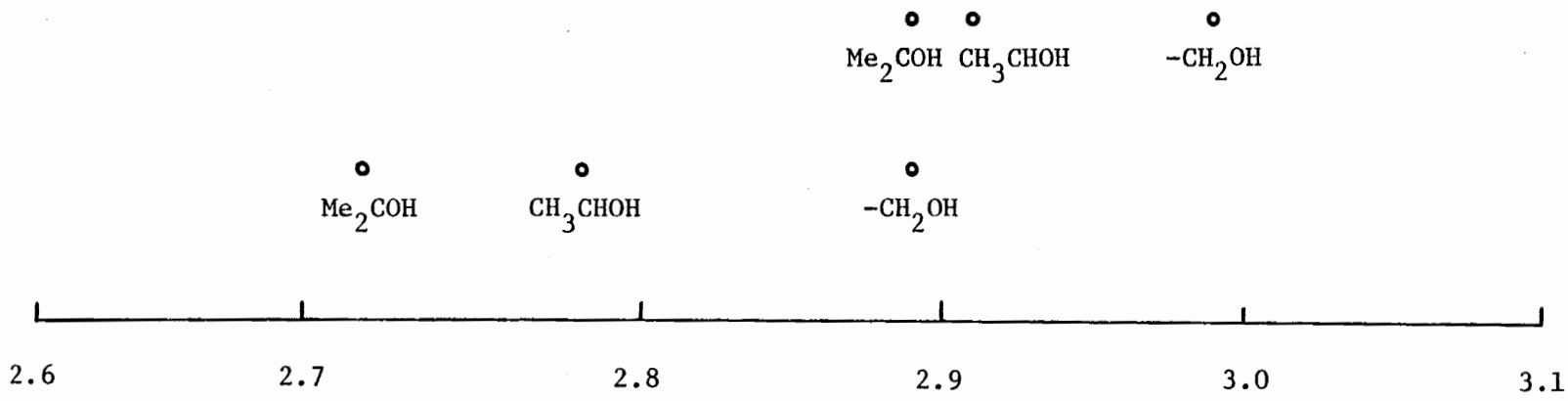

Figure 13. Plot of $a^{F_\alpha}/a^{F_\beta}_{CF_3}$ ratios for the hydroxyalkyl radical adducts of the perfluoro-olefins.

CONCLUSIONS

The results of our investigations on the hydroxyalkyl adducts of perfluoro-olefins confirmed the trends that we had observed earlier in our studies on the silyl adducts of the perfluoro-olefins. The a^{F_α} couplings became smaller and the $a^{F_\beta}_{CF_3}$ couplings increased as the free-radical adduct was made more planar by the steric strain induced by the size of the free-radical substituent. The ratio of the hfs of the α-fluorine to that of the hfs of the adjacent trifluoromethyl group were also tested as a measure of the degree of steric strain induced into the free radical. All the tests succeeded in properly ordering the substituents according to their size; although in the hydroxyalkyl free-radical adducts of perfluoropropene this result was dependent on chance to a degree because of the relatively large errors in the data. Viewed from another perspective these results suggest that possibly the failure of the a^{F_α} and $a^{F_\beta}_{CF_3}$ trends to predict the correct ordering of the triethylsilyl adducts may have been due to the long range interactions of the ethyl groups on the silyl group.

The increase in the hfs of the β-fluorines adjacent to the substituent group on the adduct, as smaller substituents are used, has proven to be a sensitive indicator of the degree of steric strain that any member of a substituent class adds to the free-radical adduct. The failure of this indicator to work in the silyl free-radical adducts of perfluoropropene may have been that the upper limit of the hfs range was reached.

The γ-fluorine hfs stayed within a narrow range of values (2.44 to 2.74 gauss). This range of values is distinctly different from the range of γ-fluorine hfs values observed for the silyl adducts, indicating that a change in the class of substituents causes a change in the spin density transmission along the carbon backbone of the adduct.

PART III

ESR STUDIES OF ADDUCTS FORMED BY THE ATTACK OF CHALCOGEN-CENTERED RADICALS ON PERFLUOROALKENES

INTRODUCTION

A number of esr studies on the hydrocarbon olefin adducts of alkoxy and thiyl radicals have been conducted.[16,29] The small number of esr studies which have dealt with group VI free-radical addition to fluorine containing olefins, have tended to restrict themselves to the simpler fluoro-olefins, with which conformational analysis is still possible.[30]

The ease with which the group VI centered radicals could be generated from the photolysis of peroxides and disulfides made them attractive as free-radical sources. Unfortunately the range over which the steric hindrance can be varied in the group VI radicals is quite limited compared to the group IV radicals discussed in the first two sections. Because of the preceding reasons a preliminary investigation was conducted with the free-radical precursors which we had available.

EXPERIMENTAL

Sample Preparation

The same procedures as in Part I were used.

Chemicals

The dimethyl disulfide and diethyl disulfide were purchased from Columbia Organic Chemicals Co. and were dried over 3 Å molecular sieves. The di-t-butyl peroxide, cyclopropane and perfluoro-olefins were treated as in Part I.

Electron Spin Resonance

The same program as in Part I was used.

Evaluation of Data

The same procedures as in Part I were used.

RESULTS

The kinetics, which are implied by our qualitative observations on the photo-irradiated systems are given below, followed by a discussion of the observed hfs. The esr spectra of primary and thiyl free radicals in nonviscous media is unable to be observed due to the extreme width of their spectral lines.[31]

MeS· and EtS· Adducts of $CF_3CF=CFCF_3$:

Suitable spectra were readily obtained, although the signal-to-noise ratios were not as large as one would have anticipated. This along with the fact that the thiyl radicals did not appear to add to the perfluoro-2-butene at low temperatures, points to a much higher activation energy for adduct formation than for the radicals studied in the first two parts of this thesis.

MeS· and EtS· Adducts of $CF_3CF=CF_2$:

Suitable spectra were not obtained.

The t-Butoxy Adduct of $CF_3CF=CFCF_3$:

The spectra did not have as good signal-to-noise ratios as the $CF_3CF=CFCF_3$ adducts in the first two parts of this thesis.

The t-Butoxy Adduct of $CF_3CF=CF_2$:

Good spectra were obtained with effort. The fact spectra were easily recorded at even -80°C shows that alkoxy radicals add more readily to perfluoro-olefins than do thiyl radicals.

The possibility that we were actually seeing the addition of a methyl radical, formed by a β-scission of the t-butoxy radical was

also considered.[33]

$$(CH_3)_3CO\cdot \longrightarrow CH_3\cdot + CH_3COCH_3$$

Figure 14. The β-scission decay reaction of the t-butoxy radical.

The β-scission process can produce a strong $\cdot CH_3$ esr signal when di-t-butyl peroxide is photo-irradiated in the presence of Freons at ambient temperature. The process is temperature-dependent however, and this is in conflict with our ability to obtain spectra at low temperatures.[34]

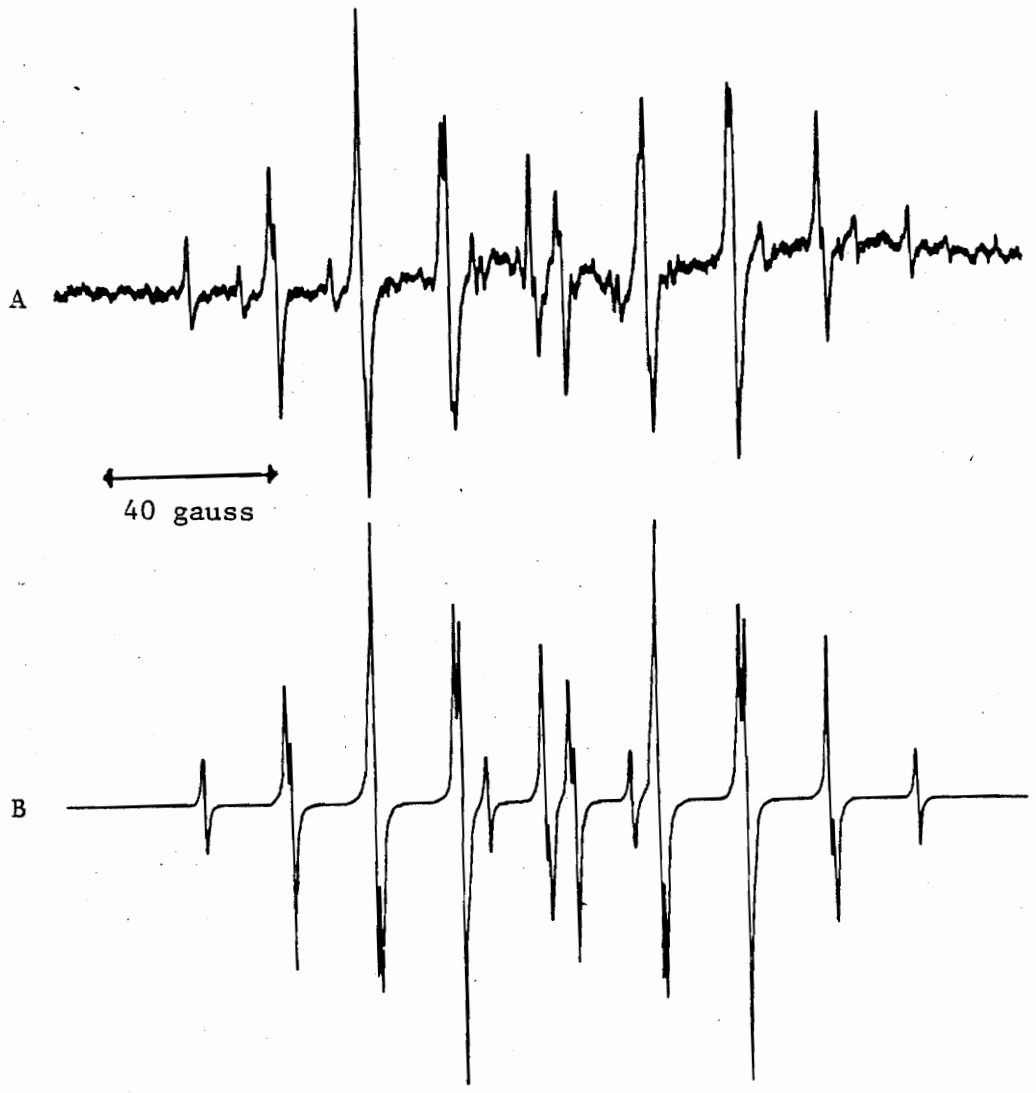

Figure 15. ESR spectra of the t-butoxy adduct of perfluoropropene. A-experimental spectrum, B-simulated spectrum.

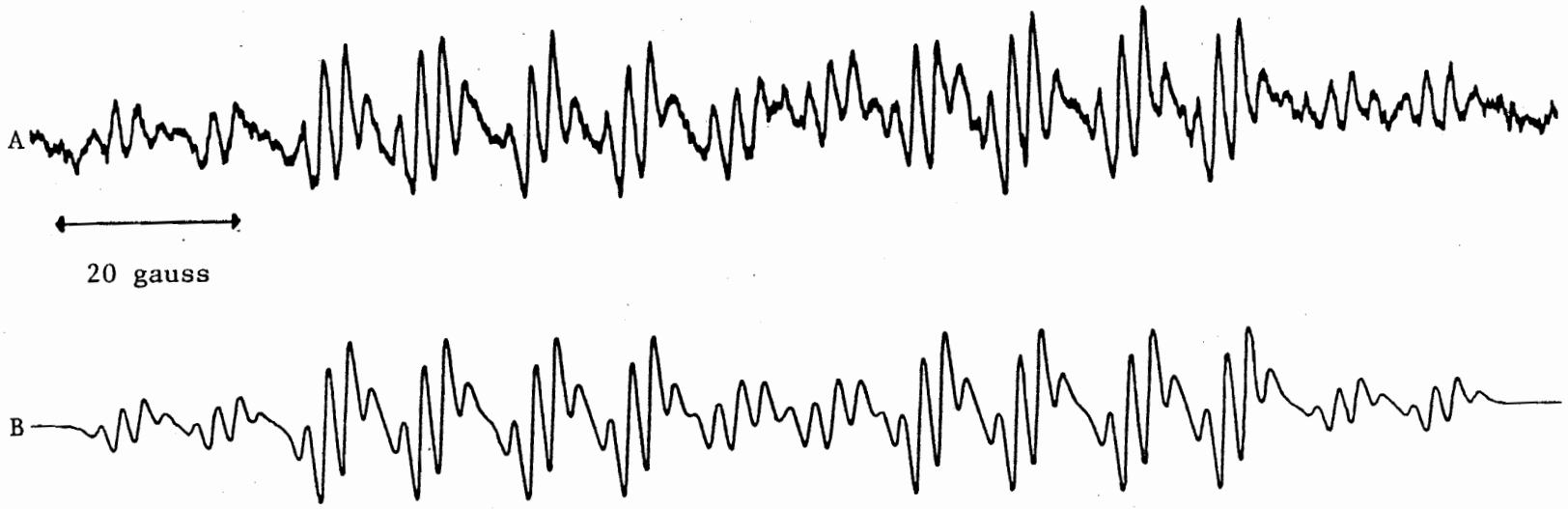

Figure 16. ESR spectra of the ethylthiyl adduct of perfluoro-2-butene. A-experimental spectrum, B-simulated spectrum.

DISCUSSION

a^{F_α} Trends:

The large values of the α-fluorine hfs which we observed in the free-radical adducts of the chalcogen-centered substituents, were due to the limited degree of steric strain that the sole alkyl group on the chalcogen center could contribute. In spite of its large t-butyl group, the t-butoxy radical adduct had a larger a^{F_α} than any of the thiyl radicals used. This was probably due to the smaller radius of the oxygen atom and possibly due in part to the greater electronegativity of the alkoxy group, which may assist in making the free radical more pyramidal.[13]

$a_{CRF}^{F_\beta}$ Trends:

The low hfs and a high temperature coefficient of about 0.04 gauss /°C indicate that the thiyl group was in a stable conformation either parallel or antiparallel to the orbital containing the unpaired electron. Incipient bonding was probably taking place between the pi orbital and a d orbital on the sulfur.

If we correct for the large temperature coefficient, the value of $a_{CRF}^{F_\beta}$ increases as we go from the ethylthiyl to the less sterically hindered methylthiyl radical. This is in keeping with the other systems we have studied.

$a_{CF_3}^{F_\beta}$ Trends:

The hfs values for the trifluoromethyl group were found to be low, as is expected for the low degree of steric strain expected

TABLE V

ESR HYPERFINE SPLITTINGS OF THE THIOL- AND ALKOXY-PERFLUORO-OLEFIN ADDUCTS[a]

Radical	Olefin	Temp., °C cor(uncor)	a^{F_α}	$a^{F_\beta}_{CF_3}$	$a^{F_\beta}_{CRF}$	a^{F_γ}	$a^{F_\alpha}/a^{F_\beta}_{CF_3}$
$\cdot OC(Me)_3$	$CF_3CF=CFCF_3$	+32(+22)	66.96[b] ±0.06	22.74 ±0.05	30.65 ±0.2	2.75 ±.04	2.95
$\cdot OC(Me)_3$	$CF_3CF=CF_2$	-23(-33)	68.98 ±0.32	21.26 ±0.06	20.12 ±0.09	----	3.25
$\cdot SEt$	$CF_3CF=CFCF_3$	+11(+1)	65.17 ±0.21	22.73 ±0.18	9.94 ±.07	2.37 ±.04	2.87
$\cdot SEt$	$CF_3CF=CFCF_3$	+27(+17)	65.11 ±0.14	22.68 ±0.11	10.54 ±0.07	2.35 ±.04	2.87
$\cdot SMe$	$CF_3CF=CFCF_3$	-11(-21)	65.57 ±0.13	22.90 ±0.09	10.27 ±0.09	2.30 ±.06	2.86

[a] In gauss.

[b] Average mean error. Absolute accuracy is about an additional 0.5% error except for the t-butoxy adduct of perfluoro-2-butene where the additional error is about 1%.

from these radicals.

a^{F_γ} Trends:

The γ-fluorine hfs for the chalcogen-centered substituents varies between 2.3 and 2.37 gauss for the thiyl adducts and is 2.75 gauss for the t-butoxy adduct of perfluoro-2-butene. These values fall within the range of values observed for the hydroxyalkyl adducts.

$a^{F_\alpha}/a^{F_\beta}_{CF_3}$ Trends:

The ratio for the ethyl- and methylthiyl radical adducts is virtually the same and indicates that there is little difference in the degree of steric strain between them. The ratio for the t-butoxy adduct is larger than that of the thiyl radical adducts and indicates the greater degree of nonplanarity at the free-radical site of the t-butoxy adducts.

CONCLUSIONS

The alkoxy and thiyl radicals do not lend themselves to showing the effects of steric hindrance in free-radical adducts. The degree of change in steric hindrance that can be utilized is quite limited limited compared to that of the silyl and hydroxyalkyl radicals we have studied. The relatively high activation energy needed for adduct formation is also a disadvantage in obtaining good spectra.

The organic peroxides offer their own special problems. The low molecular weight peroxides are explosive. The stench of the organic disulfides on the other hand, does not make one particulary eager to work with them either.

PART IV

ESR STUDIES OF PERSISTENT FREE-RADICAL ADDUCTS

INTRODUCTION

Early in our work a number of persistent free radicals were found. These ranged from the free radical adducts of perfluorobutyne with lifetimes ranging from seconds or minutes to an extremely long-lived product obtained by photo-irradiating a mixture of acetonitrile, trimethylsilane and di-t-butyl peroxide dissolved in cyclopropane, which resulted in a free radical which still gave a strong signal a year after being photo-irradiated.

Ingold and Griller were later to discover independently and publish on the nature of the free-radical adducts of perfluorobutyne.[18] They concluded that these radicals were strongly sterically hindered alkyl radicals, which resulted from a series of free-radical reactions. Their interpretation of the esr spectra in terms of two conformers of the radical (which result from the strong steric hindrance which gives the free radical its stability) is in concert with our observation that the inner and outer groups of the major quartet splitting were different but that the overall spectrum was centrosymmeteric (see Figure 17). The persistence of these free radicals goes strongly against an interpretation based on cis and trans isomers of the vinyl free radical, which is formed by the initial free-radical attack on the perfluorobutyne.

The extremely stable free radical which we produced by the photo-irradiation of a mixture a acetonitrile, di-t-butyl peroxide

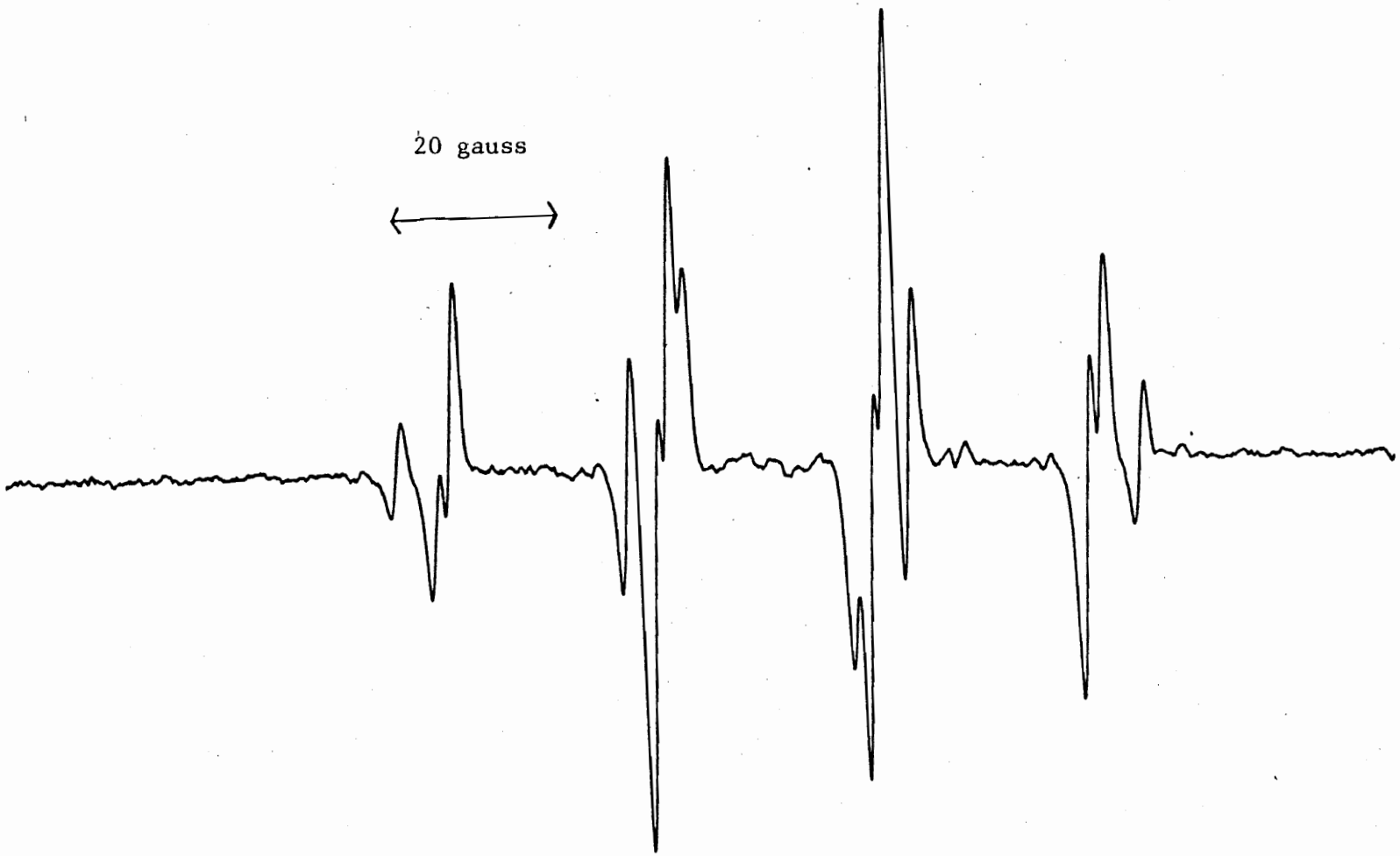

Figure 17. ESR spectrum of the $Me_3Si\cdot$ adduct of $CF_3C{\equiv}CCF_3$.

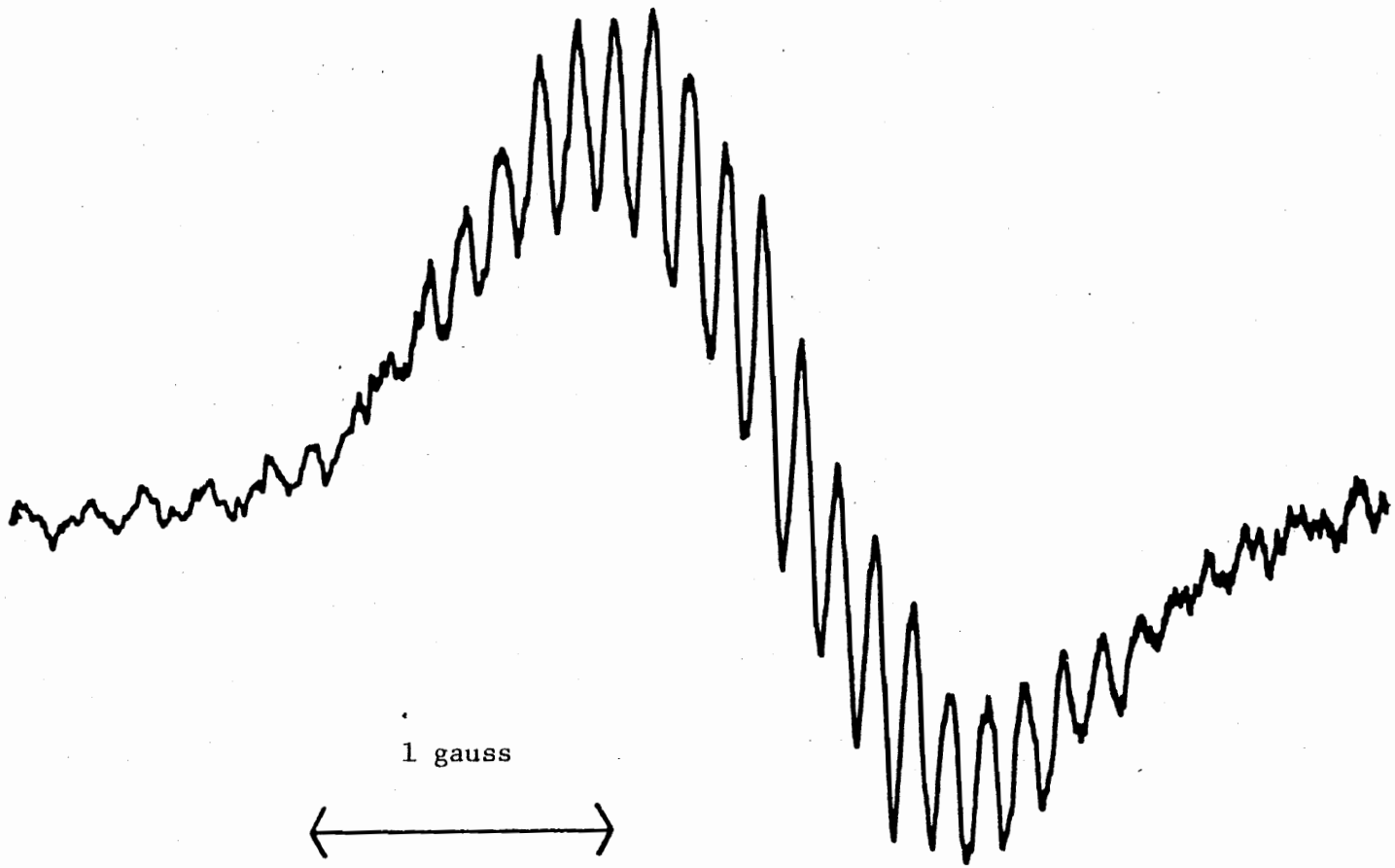

Figure 18. ESR spectrum of the 1,1,2,2-tetrakis(trimethylsilyl)ethyl radical at high resolution.

and trimethylsilane was also eventually produced and its structure elucidated by Ingold and Griller.[35] The structure was deduced to be that of the 1,1,2,2-tetrakis(trimethylsilyl)ethyl free radical and its identity was confirmed by four different synthesis.

$$(Me_3Si)_2\dot{C}HC(SiMe_3)_2$$

Figure 19. Structure of the 1,1,2,2-tetrakis(trimethylsilyl)ethyl free radical.

Besides its extremely long life, this free radical was also interesting from the standpoint of the extremely low hyperfine splitting constant which the β proton would have to have (≤ 0.27 gauss). The absence of a normal β proton hyperfine splitting (∿20 gauss) in the esr spectrum was explained in terms of the following equation.[9]

$$a^H = A + B\cos^2\theta$$

A = 0 to 5 gauss

B = ∿40 to 50 gauss

θ = the dihedral angle between the β proton and the pi orbital containing the unpaired electron.

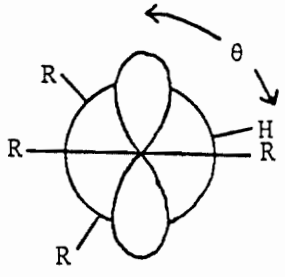

R = Me_3Si-

Ingold and Griller argued that the extreme steric hindrance which gives the free radical its persistence was also responsible for forcing it into a stable conformation where the dihedral angle between the pi orbital containing the unpaired electron and the β proton is 90°. Thus the second term of the equation is zero and this along with a very small value for the A term makes the β proton "invisible". This line of reasoning is supported by the work of Neugeberg and Groh[36], who observed abnormally small β proton splitting constants for the 1,1,2,2-tetraphenylethyl (8.45 gauss) and the 9,9'-bifluorenyl-9-yl (3.68 gauss) free radicals.

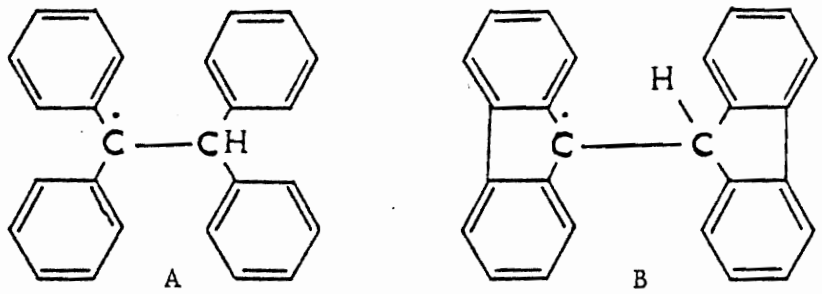

Figure 21. Structure of the 1,1,2,2-tetraphenylethyl (A) and 9,9'-bifluorenyl-9-yl (B) free radicals.

In spite of the strong evidence that Ingold and Griller have assembled to justifify their conclusions, we will attempt to show that this conclusion does not necessarily follow from the evidence which as been presented thus far. We will also suggest an alternative structure as well. In the following section we will present all the evidence that Ingold and Griller have given for their proposed structure and then follow with our own experiments and conclusions concerning the nature of this free radical.

EXPERIMENTAL

Sample Preparation

Samples were prepared and run as in our previous experimental work, except that some samples were also run without the use of cyclopropane as a diluent in order to match better the experimental conditions used by Ingold and Griller. Due to the higher dielectric losses encountered by not using a diluent, smaller esr tubes than normal had to be used in order to enable us to tune the esr cavity.

The $(Me_3Si)C{\equiv}C(SiMe_3)$ which was used was added directly to the sample tube by means of a microsyringe, due to difficulties in measuring the small quantities by the normal manometeric method. Because of its low volatility the cumyl peroxide that was used also had to be added directly to the sample tube. Whether degassing was attempted in the sample tube or was done in the one liter flask on the vacuum manifold was determined by such considerations as volatility and contamination.

Typical Sample Compositions

CH_3CN--Me_3SiH--di-t-butyl peroxide system:

CH_3CN	0.14 mmol
Me_3SiH	0.14 mmol
di-t-butyl peroxide	0.14 mmol

$(Me_3Si)C{\equiv}C(SiMe_3)$--$Me_3SiH$--dicumyl peroxide system:

$(Me_3Si)C{\equiv}C(SiMe_3)$	0.022 mmol (5 µl)
Me_3SiH	0.68 mmol
dicumyl peroxide	1.85 mmol (0.5 g)

cyclopropane 6.8 mmol

$(Me_3Si)C{\equiv}C(SiMe_3)$--$Me_3SiH$ system:

$(Me_3Si)C{\equiv}C(SiMe_3)$ 0.18 mmol (40 µl)

Me_3SiH 0.75 mmol

cyclopropane 4.8 mmol

$(Me_3Si)C{\equiv}C(SiMe_3)$ system:

$(Me_3Si)C{\equiv}C(SiMe_3)$ 0.26 mmol (60 µl)

cyclopropane 4.8 mmol

$(Me_3Si)C{\equiv}C(SiMe_3)$--$Me_3SiH$--$Me_2S_2$ system:

$(Me_3Si)C{\equiv}C(SiMe_3)$ 0.02 mmol (5 µl)

Me_3SiH 0.75 mmol

Me_2S_2 0.54 mmol

Chemicals

The use and the sources of the cyclopropane, di-t-butyl peroxide and dimethyl disulfide were the same as in the previous sections. The perdeuterated acetonitrile (Stohler Isotope Chem.) was given to us by courtesy of Dr. J.D. Graybeal.[37]

The bis(trimethylsilyl)acetylene was prepared by the method of West and Quass[38] in which tetrachloroethylene (Eastman) was reacted with a cooled mixture of lithium metal (Fisher), trimethylchlorosilane (Columbia) and tetrahydrofuran. The product was distilled twice on a spinning band column that was found to have a separating power of about ten plates when a carbon tetrachloride-benzene mixture was used to determine its separating power. The resulting product was then zone refined and the purity was determined by gas chromatography to be

better than 1 part in 8000.

RESULTS AND DISCUSSION

The Case for Ingold and Griller's Proposed Structure:

In their initial publication concerning an extremely long-lived radical which they had identified as the 1,1,2,2-tetrakis(trimethylsilyl)ethyl free radical, Ingold and Griller gave the following four routes by which they were able to obtain this free radical by photoirradiation. The source of $\underline{t}$-BuO$\cdot$ and $Me_3Si\cdot$ free radicals in all of these reactions were the following two reactions.

$$\underline{t}\text{-BuOO}(\underline{t}\text{-Bu}) \xrightarrow{h\nu} 2\underline{t}\text{-BuO}\cdot$$

$$\underline{t}\text{-BuO}\cdot + Me_3SiH \longrightarrow Me_3Si\cdot + \underline{t}\text{-BuOH}$$

A.) Me_3SiH, CH_3CN and di-$\underline{t}$-butyl peroxide: $R = Me_3Si-$

$$3Me_3Si\cdot + CH_3CN \longrightarrow CH_3\dot{C}NR_2$$

$$\underline{t}\text{-BuO}\cdot + CH_3\dot{C}NR_2 \longrightarrow CH_2{=}CRNR_2 + \underline{t}\text{-BuOH}$$

$$2Me_3Si\cdot + CH_2{=}CRNR_2 \longrightarrow RCH_2CR_2NR_2$$

$$\underline{t}\text{-BuO}\cdot + RCH_2CR_2NR_2 \longrightarrow R\dot{C}HCR_2NR_2 + \underline{t}\text{-BuOH}$$

$$R\dot{C}HCR_2NR_2 \longrightarrow RCH{=}CR_2 + \cdot NR_2$$

$$Me_3Si\cdot + RCH{=}CR_2 \longrightarrow R_2CH\dot{C}R_2$$

B.) $(Me_3Si)_2CH_2$ and di-$\underline{t}$-butyl peroxide:

$$\underline{t}\text{-BuO}\cdot + R_2CH_2 \longrightarrow R_2\dot{C}H + \underline{t}\text{-BuOH}$$

$$2R_2\dot{C}H \longrightarrow R_2CHCHR_2$$

$$\underline{t}\text{-BuO}\cdot + R_2CHCHR_2 \longrightarrow R_2CH\dot{C}R_2 + \underline{t}\text{-BuOH}$$

C.) Me_3SiH, $\underline{t}$-BuCH=CH-$\underline{t}$-Bu and di-$\underline{t}$-butyl peroxide:

$$Me_3Si\cdot + (\underline{t}\text{-Bu})CH{=}CH(\underline{t}\text{-Bu}) \longrightarrow R(\underline{t}\text{-Bu})C\dot{H}CH(\underline{t}\text{-Bu})$$

$$R(\underline{t}\text{-Bu})C\dot{H}CH(\underline{t}\text{-Bu}) \longrightarrow RCH{=}CH(\underline{t}\text{-Bu}) + \underline{t}\text{-Bu}\cdot$$

$$2Me_3Si\cdot + RCH{=}CH(\underline{t}\text{-Bu}) \longrightarrow R_2C\dot{H}CHR + \underline{t}\text{-Bu}\cdot$$

$$\underline{t}\text{-BuO}\cdot + R_2C\dot{H}CHR \longrightarrow R_2C{=}CHR + \underline{t}\text{-BuOH}$$

$$Me_3Si\cdot + R_2C{=}CHR \longrightarrow R_2C\dot{H}CR_2$$

D.) Me_3SiH, $\underline{t}$-BuC≡CH and di-$\underline{t}$-butyl peroxide:

$$Me_3Si\cdot + \underline{t}\text{-BuC}{\equiv}CH \longrightarrow R(\underline{t}\text{-Bu})C{=}\dot{C}H$$

$$R(\underline{t}\text{-Bu})C{=}\dot{C}H \longrightarrow RC{\equiv}CH + \underline{t}\text{-Bu}\cdot$$

$$3Me_3Si\cdot + RC{\equiv}CH \longrightarrow R_2C\dot{H}CR_2$$

In addition to their being able to prepare this radical by a number of different routes, their confidence in a 1,1,2,2-tetra-substituted ethyl free radical structure was further increased by the presence of Si^{29} hyperfine coupling contributions in the ESR spectra. These Si^{29} hyperfine coupling contributions are quite evident in low resolution spectra of the free radical, where a single intense peak with a pair of well resolved peaks on both sides of it is observed. The intensities and positions of these lines correspond to two non-equivalent pairs of silicon atoms ($a^{29}Si_\beta$ = 13.71 gauss, $a^{29}Si_\gamma$ = 27.59 gauss).

Up to this point we are in complete agreement with their deductions; that is to say the structure of the observed radical is that of a substituted ethyl free radical having two trimethylsilyl groups on each carbon atom. However, Ingold and Griller go on to claim that the third remaining group on the β-carbon is a hydrogen atom with an

extremely small ESR hyperfine coupling constant. Their justification of this claim is based on the following points:[35]

1.) A mechanism can be given for each of the aforementioned preparative procedures which will result in the claimed product.

2.) The following four combinations of proton coupling constants will simulate the experimential spectrum very well.

Hpp = 0.1 gauss and $a^{13}C(6^{13}C)$ = 4.88 gauss

A. $a^{H}(9H) = 0.135$, $a^{H}(9H) = 0.270$, $a^{H}(1H) = 0.675$

B. $a^{H}(9H) = 0.135$, $a^{H}(9H) = 0.405$

C. $a^{H}(10H) = 0.135$, $a^{H}(9H) = 0.405$

D. $a^{H}(9H) = 0.135$, $a^{H}(9H) = 0.405$, $a^{H}(1H) = 0.27$

The first of these combinations can be eliminated, however, since the preparation of the free radical by method A (Me_3SiH,CH_3CN and di-t-butyl peroxide) results in an unresolvable single line with a Hpp of 0.48 gauss if the trimethylsilane which is used has had the protons on its methyl groups replaced by deuterium. Since the unique proton in the first esr hyperfine combination has a value of 0.675 gauss by itself, the first combination must be rejected leaving only combinations with a β-H having a coupling constant of 0.27 gauss or less.

The extremely low value of the β-H coupling constant is explained by Ingold and Griller as being due to the poor spin coupling between the pi orbital containing the unpaired electron and the β-H, since they are in a stable conformation in which they are perpendicular to each other. This suggested conformation is supported by the large value of the Si^{29} hfs. An additional factor which may serve to lower the value

of the β-H coupling constant is the delocalization of the unpaired electron density into the Si d orbitals.[35]

The Case Against Ingold and Griller's Proposed Structure:

Ingold and Griller's synthesis of this extremely persistent free radical by four different methods appears at first glance to be a strong proof for their proposed structure. However we must ask ourselves if any of these syntheses meet the critera for the proof of a structure by independent synthesis. In order for an independent synthesis to be accepted as a valid proof of structure the reaction steps must unambiguously lead to the product in question. That is to say, a chemist familiar with the reactions involved should be able to predict the product a priori.[32]

Now admittedly, Ingold and Griller's proposed reaction steps are reasonable, but would a chemist unfamiliar with their work have agreed on the end product, given only the knowledge that the product of interest would be extremely stable and have two nonequivalent pairs of silicon atoms present, of which one pair would be on the carbon atom α to the free radical site and the other pair on one or another β-carbon atoms. Although we ourselves were quite skeptical about this proposed "esr invisible" β-H, after being exposed to Ingold and Griller's four fold syntheses and proposed mechanisms, we found it quite difficult to arrive at an alternative explaination of their experimental data.

If rather than stopping the suggested reaction mechanisms at the stage of the proposed product, we allow the product to react further, an alternative propuct becomes apparent. The free radical which has

been proposed by Ingold and Griller can combine with a t-butoxy free radical or perhaps even a methyl group produced by the β-scission decay of a t-butoxy free radical. The resulting penta-substituted ethane can then lose its sole remaining proton to a t-butyl free radical to form a free radical, which would be stabilized by steric hindrance to a remarkable degree.

$$R = Me_3Si-$$

$$t\text{-BuO}\cdot + R_2\dot{C}HCR_2 \longrightarrow R_2CHC(t\text{-BuO})R_2$$

$$t\text{-BuO}\cdot + R_2CHC(t\text{-BuO})R_2 \longrightarrow R_2(t\text{-BuO})\dot{C}CR_2 + t\text{-BuOH}$$

Figure 22. Reaction mechanism for the formation of the alternative to Ingold and Griller's stable free radical.

Although the above reaction steps serve to illustrate how a possible alternative product may be formed, the last step in the formation process is not favorable due to the steric crowding around the hydrogen to be abstracted. A more likely step would be the addition of a free radical to an appropiate tetra-substituted ethylene intermediate.

Having proposed an alternative structure, we proceeded to conduct some experiments that would show if the β-H, which had been put forward by Ingold and Griller, could be detected or be shown to be absent. Toward these ends we thought it would be interesting to see what would happen to the esr spectrum of the free radical if the proposed β-H was replaced with a deuterium atom. This experiment was easily accomplished by photolyzing a mixture of trimethylsilane, di-t-butyl peroxide and deuterated acetonitrile. The resulting esr spectrum was the same as the one produced by using ordinary acetonitrile in the reaction mixture.

However, this does not mean that the esr hyperfine contribution

associated with the β-H, if it were present, would have to have been less than 0.135 gauss (the smallest line splitting in the esr spectrum). If we assume the hfs of the β-H to be even as large as 0.27 gauss, the hfs of the analogous deuterium atom would only be expect- to be about 0.031 gauss based on a ratio of 6.5 between the magnetogyric ratios of hydrogen and deuterium. Since the peak-to-peak linewidth of the spectrum is only about 0.1 gauss, this would only cause a small decrease in the width of the spectrum and a small increase in the peak-to-peak width. Since the spectrum consists of a multitude of evenly spaced lines which gradually decrease in amplitude in the wings a small change in overall spectrum width is difficult to observe. In addition, small changes in temperature, dielectric constant of the sample or microwave power level also cause quite noticeable changes in the appearance of the spectrum as they change the peak-to-peak width of the lines.

In another experiment we tried to prepare the extremely stable radical by a route that would not involve having a proton on the ethane backbone in any of the intermediate stages. The procedure used was the photolysis of a mixture of trimethylsilane, di-t-butyl peroxide, and $(CH_3)_3SiC{\equiv}CSi(CH_3)_3$ which had been carefully fractionally distilled on a spinning band column and then further purified by zone refining in order to avoid any impurities which might have a proton present on a carbon atom which would eventually be in the ethane backbone of the stable radical. The photo-irradiation of the above mixture yielded the radical as expected but the results were not conclusive in dis-

proving their hypothesis since we had overlooked the fact that intermediates of the stable free radical could abstract a hydrogen atom from the trimethylsilane which was present and thus invalidate the whole experiment.

Ingold and Griller were later to publish on having produced their radical by three more new methods one of which was the foregoing procedure.[18] The second new method involved the attack of the trimethylsilyl radical on $Me_3CC{\equiv}CCMe_3$. The t-butyl groups on the di-t-butylacetylene are removed by a free radical β-scission process as the trimethylsilyl radical attacks and forms unstable intermediates. This method is similiar to one of their older methods which employs propyne instead of 2-butyne as a starting material. The third new method is the most direct of the procedures to date: in it the stable free radical is claimed to be formed by the simple abstraction of a hydrogen atom from $(Me_3Si)_2CHCH(SiMe_3)_2$ by a t-butoxy free radical.

Although this new method is far more direct that the previous ones, it still does not conclusively prove the structure of the stable species which is observed. As in all the other cases the possibility of the substitution of the β-H by other groups still exist. The quenching of Ingold and Griller's proposed radical by a t-butoxy free radical followed by the removal of the sole remaining proton on the ethane backbone of the molecule could have yielded an alternative free radical species.

Another approach we tried in attempting to test Ingold and Griller's proposed structure was the substitution of dicumyl peroxide

for di-t-butyl peroxide in the reaction involving the attack of $Me_3SiC{\equiv}CSiMe_3$ by $Me_3Si\cdot$ free radicals. It was hoped that a perturbation of the spectrum might be evident if the t-butoxy group in our proposed structure for the stable radical was substituted by a cumoxy group.

The dicumyl peroxide proved to be a very convenient free radical source since it was completely soluble in the cyclopropane solvent and the absorption of ultraviolet light by its phenyl groups did not appear to hinder the cleavage of its peroxide bond; indeed the sample gave a fairly intense esr spectrum attributable to the fairly stable vinyl free radical intermediate even before being photo-irradiated with the mercury capillary lamp. Apparently the fluorescent lighting was sufficient to obtain a good esr signal.

On further photo-irradiation the vinyl free radical intermediate disappeared and the esr spectrum of Ingold and Griller's stable free radical took its place. Although this result favored Ingold and Griller's position it was still far from decisive since there is a fair degree of similarity between the steric effects of the t-butoxy and the cumyl group.

Realizing the inherent weakness of the above approach in deciding the issue, if only the same spectrum were seen as other peroxides were tried, it was decided to approach the problem from another direction. If a method could be found that avoided the use of peroxides all together and still yielded as esr spectrum identical with the esr spectrum of Ingold and Griller's stable free radical the issue would be

decisively tilted in favor of Ingold and Griller's proposed structure.

After thinking along such lines it was decided that the photo-irradiation of a mixture of trimethylsilane and bis(trimethylsilyl)-acetylene dissolved in cyclopropane might yield an unambiguous result. The initial free radical precursor of the reaction would be the triplet state of the silylated acetylene. The reaction would proceed as follows.

where R = $Me_3Si\cdot$

$$RC{\equiv}CR \xrightarrow{h\nu} R\dot{C}{=}\dot{C}R$$

$$Me_3SiH + R\dot{C}{=}\dot{C}R \longrightarrow RHC{=}\dot{C}R + Me_3Si\cdot$$

$$Me_3Si\cdot + RC{\equiv}CR \longrightarrow R_2C{=}\dot{C}R \text{ (stable intermediate)}$$

$$Me_3SiH + R_2C{=}\dot{C}R \longrightarrow R_2C{=}CHR + Me_3Si\cdot$$

$$Me_3Si\cdot + R_2C{=}CHR \longrightarrow R_2CH\dot{C}R_2$$

Upon photo-irradiation, the sample gave a strong esr signal which was attributable to the 1,2,2-tris(trimethylsilyl)vinyl radical. However, strong prolonged irradiation did not make the reaction proceed further. The above results are interesting since the addition of silyl compounds to triple bonds by photoylsis is usually written without showing the free-radical intermediates, thus implying that the solvent cage process dominates the reaction to such a extent that significant concentrations of free radicals never exist.

Examination of the photo-irradiated sample after two days of aging showed the spectrum of Ingold and Griller's radical, although, of course, at a much lower intensity than that of the initial free-

radical intermediate. Even though this result strongly favors Ingold and Griller's proposed structure, it is not without its short comings.

The shape and resolution of the esr spectra were highly susceptable to change as the microwave power was changed. This was particularly true at lower power levels where modulation sidebands became apparent and made complete and detailed agreement between samples virtually impossible

A much more important criticism is the possibility that the silylated acetylene starting material may have been contaminated with oxygen, either as a loosely bound complex or as an oxygen-containing impurity resulting from the excitation of the acetylenic triple bond to a triplet state by the ultraviolet light from the fluorescent lighting and subsequent combination with molecular oxygen.

The end result of such oxygen contamination could be the creation of a $-OSiMe_3$ group β to the site of the unpaired electron and the exertion of approximately the same amount of steric hindrance as a t-butoxy group exerts. Such a species could show the same esr spectrum as the species where a t-butoxy group is β to the unpaired electron.

In order to avoid the problem of the possible similarity of esr results between different free-radical species which differ only in the steric effects of different alkoxy groups located on the carbon atom β to the unpaired electron we decided to see what would happen if the peroxide free-radical precursors were replaced by dimethyl disufide. The difference in electronegativity between these two

classes of groups should be sufficient to observe a difference in the esr spectra of their adducts.

When a mixture of Me_2S_2, $Me_3SiC{\equiv}CSiMe_3$ and Me_3SiH dissolved in cyclopropane was irradiated no significant esr signal was obtained, not even that of the 1,2,2-tris(trimethylsilyl)vinyl free radical. One possible explaination of this result was that the MeS• radical can not abstract a silyl proton nor add to a silylated acetylene but can add readily to any 1,2,2-tris(trimethylsilyl)vinyl free radical which could be formed directly from the Me_3SiH and $Me_3SiC{\equiv}CSiMe_3$ alone.

Some Comments on the Satellite Peaks of Ingold and Griller's Radical

In listing the additional peaks due to the esr active nuclei such as Si^{29} and C^{13}, Ingold and Griller mention four sets of additional peaks. These are the two doublets (13.7 and 27.6 gauss) which are attributed to two nonequivalent pairs of Si atoms and the two doublets associated with C^{13} coupling (4.9 and ∿28-29 gauss) from the α-trimethylsilyl groups and the free-radical center respectively. The uncertainty in the C^{13} coupling value for the free-radical center is due to the fact that it is unresolved.

Upon close examination of the Si^{29} satellite peaks we were struck by the fact that the outer Si^{29} satellite peaks are fairly well resolved into hyperfine peaks but that the inner Si^{29} peaks are poorly resolved. This suggested that the a C^{13} peaks were under the inner set of Si^{29} peaks and had an anomalously low esr hfs.

The examination of a sample prepared by photo-irradiating a mixture of di-t-butyl peroxide, acetonitrile and trimethylsilane, however, showed that numerous peaks due to other stable free radicals were present even after aging at room temperature. This fact, coupled with the fact that the $a^{13}C_{\alpha}$ of $(Me_3Si)_3C\cdot$ has a value of $\sim$26 gauss has led us to the conclusion that the $a^{13}C_{\alpha}$ peaks are most likely hidden under the outer Si^{29} peaks and possibly even have their fine structure in phase with that of the fine structure of the Si^{29} peaks so as to avoid interfering with the high resolution which is obtained. On this basis the peaks which interfere with the resolution of the inner Si^{29} peaks are probably due to a stable free-radical impurity. These conclusions explain why the innermost doublet was the smaller of the set by about 6%.

It should also be pointed out that the peak-to-peak height ratios between the main peak and the observed Si^{29} satellite peaks expected for natural abundance Si^{29} was not seen but instead was off by about 30%. The degree of variance in the ratios appeared to be affected by the power level used while scanning the spectra. This discrepancy is easily accounted for by the expected non-linearity of the amplification of peaks which differ 20-fold in amplitude. Similar effects are well known in nmr spectroscopy.

CONCLUSIONS

From the experiments done to date the most probable structure for this persistent free radical appears to be Ingold and Griller's proposed structure. However, before we become too content with their proposed structure we should take heed from the foregoing discussion which illustrates the difficulty in proving the structure of an esr species and the ease with which one can be led to the wrong conclusions.

In spite of the potential problem of elucidating their structures, the study of persistent free radicals holds promise. The studies of Ingold and Griller show the diversity and ease of formation of such species.

The ability to examine these species easily at high concentration and high resolution offers us the opportunity to study the esr coupling effects of isotopes of low abundance and the line-broadening effects due to the spin-spin interactions between free radicals as a function of concentration, temperature and the viscosity of the solvent. The possibility of isolating some of the more persistent free radicals offers the possibility of highly selective free-radical chemical reagents as well as the possibility of observing new decay mechanisms and rearrangements.

BIBLIOGRAPHY

1. R. W. Fessenden and R. H. Schuler, J. Chem. Phys., 33, 935 (1960).

2. W. T. Dixon and R. O. C. Norman, J. Chem. Soc. (London), 3119 (1963).

3. R. Livingston and H. Zeldes, J. Chem. Phys., 44, 1245 (1965).

4. J. Q. Adams, J. Amer. Chem. Soc., 90, 5363 (1968).

5. P. J. Krusic and J. K. Kochi, J. Amer. Chem. Soc., 90, 7157 (1968).

6. M. V. Merritt and R. W. Fessenden, J. Chem. Phys., 56, 2353 (1972).

7. L. C. Duncan and G. H. Cady, Inorg. Chem., 3, 850 (1964).

8. J. R. Morton and K. F. Preston, J. Chem. Phys., 18, 98 (1973).

9. H. Fischer, Z. Naturforsch., 20a, 428 (1965).

10. R. W. Fessenden and R. H. Schuler, J. Chem. Phys., 43, 2704 (1965).

11. H. Konishi and K. Morokurma, J. Amer. Chem. Soc., 94, 5603 (1972).

12. L. Pauling, J. Chem. Phys., 51, 2767 (1969).

13. R. V. Lloyd and M. T. Rogers, J. Amer. Chem. Soc., 95, 1512 (1973).

14. J. March, "Advanced Organic Chemistry: Reactions, Mechanisms and Structures", McGraw Hill Book Company, New York, N. Y., (1968).

15. W. A. Pryor, "Introduction to Free Radical Chemistry", Prentice-Hall Inc., Englewood Cliffs, N. J., 1966, p 56.

16. P. J. Krusic and J. K. Kochi, J. Amer. Chem. Soc., 93, 846 (1971).

17. E. W. Stone and A. H. Maki, J. Chem. Phys., 38, 1999 (1963).

18. D. Griller, J. W. Cooper and K. U. Ingold, J. Amer. Chem. Soc., 97, 4269 (1975).

19. J. E. Wertz and J. R. Bolton, "Electron Spin Resonance", McGraw Hill Book Company, New York, N. Y., 1972, p 124.

20. K. S. Chen and J. K. Kochi, J. Amer. Chem. Soc., 96, 1383 (1974).

21. P. Laszlo and P. J. Stang., "Organic Spectroscopy: Principles and Applications", Harper and Row, New York. N. Y., 1971, pp. 34-35.

22. W. T. Dixon and R. O. C. Norman, J. Chem. Soc., 3119 (1963).

23. R. Livingston and H. Zeldes, J. Chem. Phys., 44, 1245 (1966).

24 J. Q. Adams, J. Amer. Chem. Soc., 90, 5363 (1968).

25. W. H. Urry, F. W. Stacey, O. O. Juveland and C. H. McDonnell, J. Amer. Chem. Soc. 75, 250 (1953).

26. J. D. LaZerte and R. J. Koshar, J. Amer. Chem. Soc., 77, 910 (1955).

27. R. F. Stockel and M. T. Beachem, J. Org. Chem., 32, 1658 (1967).

28. H. Muramatsu, K. Inukai and T. Ueda, J. Org. Chem., 30, 2546 (1965).

29. K. S. Chen and J. K. Kochi, J. Amer. Chem. Soc., 96, 1383 (1974).

30. K. S. Chen, P. J. Krusic and J. K. Kochi, J. Phys. Chem., 78, 2030 (1974).

31. M. C. R. Symons, J. Amer. Chem. Soc., 91, 5924 (1969).

32. R. B. Bates and J. P. Schaefer, "Research Techniques in Organic Chemistry", Prentice-Hall, Englewood Cliffs, N. Y., 1971, p 123.

33. W. A. Pryor, "Introduction to Free Radical Chemistry", Prentice-Hall, Englewood Cliffs, N. J., 1966, p 22.

34. P. J. Krusic, Central Research Dept., Wilmington, Delaware, E. I. du Pont de Nemours and Company, personal communication.

35. D. Griller and K. U. Ingold, J. Amer. Chem. Soc., 96, 6203 (1974).

36. F. A. Neugebauer and W. R. Groh, Tetrahedon Lett., 12, 1005 (1973).

37. J. D. Graybeal, Virginia Polytechnic Institute and State University, 1974.

38. R. West and L. C. Quass, J. Organometal. Chem., 18, 55 (1969).

APPENDIX

Basic Outline of Equipment

A Varian E-12 spectrometer system was used for our studies. The esr cavity was modified to permit the photolytic generation of free radicals directly in the cavity. A low dielectric loss suprasil quartz insert Dewar was made to allow low temperature studies to be conducted. The temperature of the insert Dewar was regulated by a Varian nmr temperature controller.

A water cooled mercury capillary lamp with a suprasil quartz optical system was used as the ultraviolet light source. The power for the lamp was provided by a one kilowatt constant wattage transformer with a variac input.

ESR Spectrometer System

A Varian E line series esr spectrometer employing a Varian E-101 microwave bridge and a Varian 12-inch high field electromagnet (V-HF 3900 series) was used for the study. The Varian E-234 optical transmission cavity supplied with the instrument had two ports on the front and back. Each port consisted of a mounting plate joined to a two inch length of 1/4 x 1/2 inch waveguide. We found that the light transmission characteristics could be vastly improved by replacing the front light transmission end plate with a 1 x 1 5/8 x 1/32 inch gold plated brass grid. The grid consisted of ten slots 0.064 inch high and 0.4 inch long. The remaining metal between the slots was 0.016 inch high, resulting in a grid with a 80% open area. In order to achieve a good electrical

contact of the grid to the cavity with mininium distortion, a 1 x 1 5/8 x 1/4 inch pressure plate was placed over the borders of the grid. The sides of the rectangular opening in the pressure plate were given an outward taper in order to avoid blocking portions of the converging light beam from entering the cavity. Since the rear light transmission end plate was extraneous and decreased the Q of the cavity, it was replaced by a 0.275 x 1.024 x 1.634 inch gold plated brass plate.

In assembling the front and rear of the cavity, care must be used to progressively tighten the screws in the proper sequence (e.g. top-left to bottom-right to top-right to bottom-left) till they have been brought to the proper torque. If after reassembling the cavity, a poor signal-to-noise ratio is obtained from a suspected warping of the cavity, loosen the screws and retighten in the forementioned manner. But under no circumstances should the side plates of the cavity be removed. To do so will result in the distortion of the cavity. Unnecessary removal and reassembly of the front and rear sections of the cavity are also to be avoided, as this will result in the deterioration of the silver gaskets, which form the electrical connection between the main body of the cavity and the front and back plates. When in use the cavity should be continuously purged with dry nitrogen, via the nipple on the top of the waveguide. Failure to do so may result in the contamination of the cavity by dust or in the condensation of moisture inside the cavity if the insert Dewar is in use.

Calibration of ESR Spectrometer

Upon running spectra of a dilute alkaline solution of Fremy's salt ($(KSO_3)_2NO$) at various portions of the 200 and 400 gauss scan ranges of the esr spectrometer, it was noticed that the value of the observed esr nitrogen hyperfine splitting constant increased as one offset the spectra further from the center of the scale. The increase in the hyperfine splitting values was roughly linear as one moved off the center of the scale, except for an abrupt decline on the extreme left of the scale. Recycling the magnetic field to a low value before a scan didn't seem to affect this abrupt decline. Thus the abnormality didn't appear to stem from any simple hysteresis of the magnet.

This nonlinearity is believed to arise from the nonlinearity of the Hall device used to track the magnetic field. In order to correct for this nonlinearity we derived a correction formula in the following manner.

The relative size of the nitrogen hyperfine splitting constant of Fremy's salt as compared to it's extrapolated value in the center of the spectrum is given by:

$$S_R = \left(1 + \frac{X \cdot C}{100 X_{Total}} \right)$$

Where S_R is the relative size of the nitrogen hyperfine splitting, C the percentage increase in the splitting constant as measured from the extrapolated values at the center and edges of the spectrum, X the distance from the center, and X_{Total} the distance

from the center to the edge. To obtain the cumulative effect of the nonlinearity we intergate the above formula with respect to X and get the formula below.

$$X_{Exp} = \int_0^X \left(1 + \frac{X \cdot C}{100 X_{Total}} \right) \, dX$$

$$X_{Exp} = X + \frac{X^2 C}{200 X_{Total}}$$

Where X is the true value of a position relative to the center of a spectrum and X_{Exp} is the actual measured value. By use of the quadratic equation we obtain the required correction formula.

$$X = \frac{\sqrt{1 + (.02/X_{Total})CX_{Exp}} - 1}{(.01/X_{Total})C}$$

By combining the constants the equation simplifies to the equation below.

$$X = \frac{\sqrt{1 + AX_{Exp}} - 1}{B}$$

Where A and B are the new constants resulting from the combining process. The experimential values of the nitrogen hyperfine splittings of a dilute solution of Fremy's salt which were taken at various positions using the 200 and 400 gauss scan ranges (Table VI) were fitted to a best line least squares fit. The slopes of the best lines fits were then used to obtain the C parameter for the left and right sides of the 200 and 400 gauss scan ranges (Table VII). The use of the above equation in correcting experimental data resulted in a vast improvement in the esr simulations.

TABLE VI

NITROGEN HYPERFINE SPLITTING OF A .001 MOLAR SOLUTION[a] OF FREMY'S SALT AS A FUNCTION OF POSITION ON THE 200 AND 400 GAUSS SCAN RANGES

200 Gauss Scan Range:

To Left of Center		To Right of Center	
Position[b]	a_N x 0.5	Position[b]	a_N x 0.5
8.1	12.35	3.0	12.4
13.1	12.4	4.2	12.35
25.5	12.4	15.5	12.65
41.75	12.6	31.85	12.6
54.35	12.6	44.5	12.65
70.95	12.8	60.9	12.65
72.6	12.75	69.0	12.65
83.65	12.6	73.6	12.75
85.3	12.65	81.7	12.75

400 Gauss Scan Range:

To Left of Center		To Right of Center	
Position[b]	a_N x 0.5	Position[b]	a_N x 0.5
0.1	12.5	0.5	12.55
1.25	12.4	4.05	12.45
14.4	12.45	4.1	12.45
14.6	12.45	4.5	12.5
14.95	12.35	4.7	12.45
15.0	12.45	23.3	12.55
33.8	12.5	23.4	12.65
34.1	12.5	23.7	12.7
34.1	12.6	23.8	12.7
34.1	12.5	42.6	12.6
53.1	12.65	42.8	12.7
53.4	12.7	43.05	12.7
53.4	12.65	43.2	12.6
53.45	12.75	62.0	12.6
72.7	12.8	62.1	12.65
72.8	12.75	62.4	12.7
72.9	12.8	62.6	12.7
73.1	12.7	81.4	12.75
		81.6	12.85
		81.9	12.9
		82.0	12.75

[a] 10% Na_2CO_3 solution

[b] units: 1/200's of total scan

TABLE VII

RESULTS OF THE LEAST SQUARES BEST LINE FIT OF THE SCAN RANGE NONLINEARITY DATA[a]

	Intercept	Slope	Error in Y	Value of Y at End of Scale	%Increase at End of Scale
Left Side of 200 Gauss Range	12.34 ±0.06	.0045 ±.0011	±0.089	12.79	3.6 %
Right Side of 200 Gauss Range	12.43 ±0.05	.0042 ±.0009	±0.081	12.85	3.4 %
Left Side of 400 Gauss Range	12.38 ±0.03	.0053 ±.0006	±0.060	12.91	4.3 %
Right Side of 400 Gauss Range	12.50 ±0.03	.0035 ±.0006	±0.072	12.85	2.8 %

[a]See Table

The scaling factors needed to obtain absolute values on the 200 and 400 gauss scales were obtained using a 1×10^{-3} molar manganese (II) chloride solution. The manganese (II) chloride esr data used to calculate these scaling factors was obtained courtesy of Dr. Paul J. Krusic (Central Research Department, E. I. du Pont de Nemours, Wilmington, Delaware) who used an esr spectrometer employing an nmr water marker to gather the data.

In the case of some older data an additional scaling factor had to be used to make it consistent with the newer data. Each time the Hall device is repositioned the range scale should be recalibrated. Since the sensitivity of the Hall device varies as a function of its orientation in the magnetic field, care should be used to place it reasonably perpendicular to the magnetic field.

In comparing the work of different authors in the esr literature, it should be kept in mind that failure to calibrate properly is probably the greatest single factor in the lack of consistency between their results, instead of differences in temperature and solvent as is often presumed. This is particularly evident if one attempts to find a correction factor to correlate their works.

Temperature Regulation System

A Varian V-6040 nmr variable temperature controller was used to regulate the temperature of the sample. The temperature of the sample was monitored with a copper-constantan thermocouple positioned 1 cm inside of the top of the insert Dewar. The thermocouple

potential was measured with a Keithley 160 digital multimeter. Frequent stirring of the ice bath reference was avoided by starting with a low water level and placing an excess of ice in the Dewar to keep the ice forced to the bottom. A glass collar 35 mm high and 20 mm wide at the top was placed over the top of the cavity to partially insulate and keep frost away from the top of the insert Dewar.

The Varian Insert Dewar supplied with the instrument developed a strong hydrogen atom esr signal after prolonged ultraviolet irradiation. To overcome this problem an insert Dewar was fabricated from Suprasil grade quartz (Amersil Inc., 685 Ramsey Ave., Hillside, N. J.) by our glass blowing shop. The Suprasil tubing was etched to a thickness of approximately 0.3-0.4 mm by the use of concentrated reagent grade hydrogluoric acid at 80°C. As a result of this extreme thinness the reduction of the Q of the esr cavity due to the insert Dewar is negligible. This is in sharp contrast to the loading effects of the original insert Dewar.

The 11.4 mm outer diameter of the insert Dewar balances ease of insertion and removal from the esr cavity (I.D. 11.6 mm) with a minimum risk of breakage. The surface tension of the quartz during construction had caused a contraction of the lip of the insert Dewar that could only be partly corrected by grinding. Unfortunately this resulted in the effective reduction of the inside diameter of the insert Dewar since the lip had an I.D. of only 8.0 mm.

Mercury Capillary Lamps

The light source used was a C-1-B mercury capillary lamp manufactured by P.E.K. (825 E. Evelyn Ave., Sunnyvale, Calif. 94086).

The ability of the C-1-B lamps to operate in a vertical position proved them to be better suited to our needs then the AH6-1 mercury capillary lamps which we initially used.

When we began our work we had difficulty from white deposits which would form on the inside of the quartz envelopes of the lamps near the electrodes. These deposits would grow with use until a crack would occur. Correspondence with the lamp manufacturer showed these deposits to be due to the devitrification of the quartz due to excessive cooling. Reduction of the lamp water flow to 5 quarts per minute effectively removed this difficulty.

Experience also showed that decreasing the voltage to the primary of the constant wattage transformer powering the lamp to a range of 95 to 105 volts, helped not only to increase the lifetime of the lamps but increased the arc stability as well. Our initial explanation of the increase in arc stability was that a decrease in the current though the lamp resulted in a lessening of the interaction between the arc and the magnetic field. However the output meters of the power supply showed that as the voltage to the primary of the constant wattage transformer was decreased the output current to the lamp remained virtually unchanged while the voltage drop across the lamp decreased. In light of this observation, it is now believed that the decreased tendency of the lamp to flicker on and

off is due to the decrease in the heating of the lamp electrodes which results in a lessening of the tendency of the mercury to break free from the upper electrode.

In order to counter the destabilizing influence of the 600 gauss magnetic field acting upon the lamp, a set of ferrite ceramic magnets (Edmund Scientific Co., No. P-60,528) were mounted about the lamp. These magnets were chosen in spite of their brittleness and difficulty in machining, since they were the only readily available magnets with very high coercivity. In order to avoid thermal cracking of the magnets from the brillance of the lamp, aluminum foil was placed on the inner faces of the magnets (previous to this a lead shutter which was placed 21 mm from the water jacket of the lamp was melted by the unfocused light of the lamp.

Our final discovery involving the operation of the lamp, occurred when difficulty was encountered from the lamp flickering on and off due to the mercury in the upper portion of the lamp breaking free from the electrode. After stopping and redistributing the mercury a number of times we decided to operate the lamp without redistributing the mercury. Surprisingly such a mode of operation was not particularly detrimental to the lamp and greatly simplified our operations. It should be noted however that some mercury normally remained at the top electrode, although it is not known how important this is.

Upon aging, the lamp will become progressively harder to start. The lamp can be helped to start by touching the water inlet atop the lamp mounting with a vacuum testing coil. However in order to help avoid possible damage to the microwave detector, the microwave bridge should be switched to the standby mode.

Lamp Mounting and Cooling

The water velocity jacket for cooling the lamp had an overall length of 90 mm and the O.D. diameter of the ends was 22.7 mm. The portion of the jacket covering almost the complete length of the arc in the lamp had an inside diameter of 8 mm and was made from Suprasil grade quartz in order to provide for maximum long-term transparency in the ultraviolet region of the spectrum.

The mount which held the lamp and its water velocity jacket were purchased from Geo. W. Gates & Co., Hempstead Turnpike & Lucille Ave., Franklin Square, L. I., N. Y. In order to supply the lamp with water, the lamp mount had to be modified by epoxying aluminum blocks to the water inlet and outlet. A set of holes drilled at right angles in the blocks enabled water to be conveniently supplied to the mount. A thread webbing reinforced tubing capable of withstanding the back pressure created by the water velocity jacket was used to connect the lamp mount to an on-off valve. The water flow rate was adjusted by a faucet on the water line, which had been calibrated with the lamp in place.

A muffin fan was used to air cool the lamp housing to prevent the destruction of the bakelite portions of the lamp mounting. In order to remove the fan from the magnet field so it could operate properly, a 13 in. high wooden extension was used on the lamp housing. The interior of the lamp housing and extension was painted black to decrease the amount of stray U.V. radiation.

Optical System

The optical system consisted of a rear mirror, shutter, primary collimating lens, heat filter cell and refocusing lens. The rear mirror (Edmund Sci. Co., 41,054) had an O.D. of 52 mm and a 38 mm focal length. In using the rear mirror care should be used to not refocus the light completely back onto the lamp. The shutter consisted of a piece of sheet brass silver soldered onto a brass rod. Indentations on the rod served to mark the limits of travel and aided in positioning the shutter.

The primary collimating lens was a 1.5 inch diameter, f/1, Suprasil quartz lens. This lens should be positioned at 95% of it's focal length from the lamp to compensate for the change in the refractive index in the short wave ultraviolet region of the spectrum.

The heat filter consisted of a cell 5 cm long, which was equipped with 1.5 inch diameter Suprasil windows. A 0.1 molar nickel chloride solution was circulated though the cell by a pump (Model MDX-5, Cole Parmer Instrument Co.) into a 2 liter reservoir.

A 1.5 inch diameter, 4 inch focal length Suprasil lens was then used to refocus the light onto the sample. A 4 inch focal length was chosen since its rate of convergence was such, that the entrance of the cavity did not block out the light.

Lamp Power Supply

The power for the lamp was supplied by a one kilowatt constant wattage transformer (P.E.K.). The input to the primary side of the transformer was regulated by a variac. The primary side of the transformer was also equipped with a pilot light and a on-off switch. The power supply output was monitored with 3 amp and 1500 volt meters. The high voltage output leads plugged into porcelain feed through insulators on the lamp housing.

VITA

Richard P. Kozloski was born in Derby, Connecticut on June 25, 1946. After graduation from Notre Dame High School in West Haven, Connecticut in 1964 he attended the University of Connecticut (Storrs) and recieved a Bachelor of Arts Degree in Chemistry in 1968. In 1977 he completed the requirements for a Ph.D. degree in Chemistry at the Virginia Polytechnic Institute and State University.

Richard P. Kozloski

ESR INVESTIGATION OF SOME FREE-RADICAL ADDUCTS

by

Richard P. Kozloski

(ABSTRACT)

The effect of steric strain on the esr hyperfine coupling constants of several free-radical adducts of perfluoropropene and perfluoro-2-butene were investigated. Silyl, hydroxyalkyl, thiyl and alkoxy free radicals, which were generated by photo-irradiation, reacted with these olefins to form free-radical adducts. Trends in the esr hfs were then looked for in each class of adducts.

The thiyl and alkoxy radicals were found to be unsuitable for this type of study due to the low degree of steric strain produced by these species in the adducts. Trends toward higher $a^{F\beta}_{CF_3}$ hfs and lower $a^{F\alpha}$ hfs were observed for the silyl and hydroxyalkyl radical adducts as the steric strain in the adduct was increased. The ratio of the $a^{F\alpha}$ to $a^{F\beta}_{CF_3}$ hfs was shown to be a good measure of the degree of steric strain in these radical adducts.

The possibility that the $(Me_3Si)_2\dot{C}HC(SiMe_3)_2$ free radical, which has been reported to contain an "esr invisible" β-H, might be misidentified was investigated. Our conclusion was that the β-H is present and has not been replaced by a t-butoxy group.